UNIVERSITY OF CALIFORNIA

Los Angeles

Rigidity and Flexibility of Polyhedral Structures

A dissertation submitted in partial satisfaction

of the requirements for the degree

Doctor of Philosophy in Mathematics

by

Robert Miranda

2025

ABSTRACT OF THE DISSERTATION

Rigidity and Flexibility of Polyhedral Structures

by

Robert Miranda
Doctor of Philosophy in Mathematics
University of California, Los Angeles, 2025
Professor Igor Pak, Chair

This dissertation consists of three chapters based on papers on rigity and flexibility in polyhedral geometry.

Chapter 1 answers a question posed by Glazyrin and Pak in [GP22] of whether every integral curve is cobordant to a unit rhombus. We show this is false in the orientable case, but that every integral curve is orientably cobordant to finitely many unit rhombi. This chapter is based on the paper *Cobordism of Domes over Curves*, which is accepted to Proceedings of the AMS.

Chapter 2 introduces a generalization of planar linkages to higher dimensions, which we call *polyhedral linkages*. We prove an extension of Kempe's Universality Theorem for polyhedral linkages in all dimensions $n \geq 3$, and all linkages are embedded. This chapter is based on the paper *Universality of Polyhedral Linkages*, which is accepted to Beiträge zur Algebra und Geometrie.

Chapter 3 gives a construction for a flexible 3-periodic polyhedral surface which retains periodicity during flexion, improving a 2-periodic construction previously given by Glazyrin and Pak in the appendix of [GP22]. We first give a construction of an embedded polyhedral

linkage with the same properties, and then describe a transformation to produce a polyhedral surface. This chapter is based on an unpublished manuscript written with Alexey Glazyrin and Igor Pak.

The dissertation of Robert Miranda is approved.

Anton Bernshteyn

Joaquín L. Moraga Saez

Pavel Galashin

Igor Pak, Committee Chair

University of California, Los Angeles

2025

This work is dedicated to my wife, Sophia, who supported me throughout the whole process, and to my son, Theodore, who showed up near the end.

TABLE OF CONTENTS

LIST OF FIGURES

ACKNOWLEDGMENTS

First, I would like to sincerely thank my advisor, Professor Igor Pak, for his unwavering support. He taught me a lot about math, but perhaps more about life, and what things are important in each.

Moreover, I am grateful to my entire committee. Professor Pavel Galashin, Professor Joaquín Moraga, and Professor Anton Bernshteyn, for their mentorship, feedback, service, and review of this work. Besides serving in my committee, they have each played a unique role in guiding my path through the program and my experience would be completely different and certainly diminished without any of them.

I am also grateful to Alexey Glazyrin, with whom (along with Igor Pak) I collaborated on the work on fully flexible periodic surfaces, which is presented here in Chapter 3. Our discussions and his feedback and ideas were invaluable, in Chapter 3 but also throughout this dissertation.

And not least, to the Mathematics Department as a whole, especially the combinatorics group. In particular, to my peers Thomas Martinez, Matty Tyler, Ariana Chin, Olha Shevchenko, Ian Shors, James Leng, Nikita Gladkov, Andrew Sack, and David Soukup, who inspired and motivated me. Also to my office mates Ben Major, Fred Vu, Adam Zheleznyak, John Hopper, Emmy Van Rooy, and Zach Baugher, who were frequently my first sounding boards of sometimes good but mostly bad ideas. And the combinatorics post-docs Terrence George and Colleen Robichaux, who were excellent and supportive role models. Very little of this dissertation would have come about without such a rich mathematical community in which to learn, discuss, and think.

Chapter 1 will appear as the paper Cobordism of Domes over Curves in Proceedings of the AMS. Chapter 2 will appear as the paper Universality of Polyhedral Linkages in Beiträge zur Algebra und Geometrie. And Chapter 3 will appear as a joint paper with Alexey Glazyrin and Igor Pak which is still in preparation.

VITA

2022	B.S. with Honors (Mathematics and Computer Science), Yale University, New Haven, Connecticut.
2022 - 2025	Teaching Assistant, Mathematics Dept., UCLA, Los Angeles, California.
2023	M.A. in Mathematics, UCLA, Los Angeles, California.
2024	C.Phil. in Mathematics, UCLA, Los Angeles, California.

PUBLICATIONS

R. Miranda, Cobordism of Domes Over Curves, accepted Proceedings of the AMS.

R. Miranda, Universality of Polyhedral Linkages, accepted Beiträge zur Algebra und Geometrie.

A. Glazyrin, R. Miranda, I. Pak, Flexible Periodic Surfaces, in preparation.

CHAPTER 1

Cobordism of domes over curves

1.1 Introduction

Let γ be a closed piecewise linear curve in three dimensional Euclidean space $\mathbb{E}$. We say that γ is integral if all intervals have unit length. We also consider the case where γ has multiple connected components, in which case we say that γ is a union of integral curves. Now let S be a piecewise linear complex in $\mathbb{E}$ with boundary γ and whose facets are all unit triangles. Note that S need not be embedded or immersed. We say that S is a *dome over* γ, that γ is *spanned* by S, and that γ *can be domed*.

As early as 2005, Kenyon asked if every integral curve can be domed, see [Ken05]. In 2022, this was shown to be false by Glazyrin and Pak, who proved a necessary condition for a unit rhombus to be domed in [GP22]. Moreover, Glazyrin and Pak conjectured that this is in some sense the only restriction that prevents a general integral curve from being domed.

Conjecture 1.1.1 ([GP22, Conj. 5.14])**.** *For every integral curve γ, there is a unit rhombus ρ and a dome over $\gamma \cup \rho$.*

Formally, we say that two integral curves γ and η are *cobordant* if there is a dome over $\gamma \cup \eta$. The dome will be called a *cobordism* between γ and η. When the cobordism is orientable, we say that γ and η are *orientably cobordant*. Note that if γ and η are cobordant, then γ can be domed if and only if η can be domed, but the converse is not necessarily true. In this context, Glazyrin and Pak asked if every integral curve is cobordant to a unit

rhombus. This is false for orientable cobordisms.

Theorem 1.1.2. *There exists an integral curve γ of length 5 which is not orientably cobordant to any unit rhombus ρ.*

Our proof of this negative result is non-constructive. We show that for almost all pairs of unit rhombi ρ_1, ρ_2, the union $\rho_1 \cup \rho_2$ is not orientably cobordant to any third unit rhombus ρ_3. Then we give a cobordism between $\rho_1 \cup \rho_2$ and γ. Our work builds upon techniques introduced by Anan'in and Korshunov, who gave a second proof that Kenyon's question is false in [AK24]. Their proof is also non-constructive, and shows that almost all integral curves cannot be domed. They consider a boundary map from the moduli space of domes to the moduli space of integral curves, and prove that its image has measure zero in the orientable case. Our result extends their work by allowing unions of integral curves.

We also prove a weaker version of Conjecture 1.1.1, posed by Glazyrin and Pak in [GP22, Conj. 5.15], which allows for finitely many rhombi.

Theorem 1.1.3. *For every integral curve γ, there is a finite set of unit rhombi $\rho_1, \ldots, \rho_k$ such that γ is orientably cobordant to $\rho_1 \cup \ldots \cup \rho_k$. Moreover, for $|\gamma| = n$, it suffices to take $k = n^2 + 2n - 12$ rhombi.*

Our proof is constructive, and uses *rhombus equivalence* to reduce a generic integral curve to a planar integral curve. We use $B_r(v)$ to mean the sphere of radius $r > 0$ around a point $v \in \mathbb{E}$, and for a set of points $v_1, \ldots, v_n \in \mathbb{E}$, we use $[v_1 \ldots v_n]$ to mean the integral curve through $v_1, \ldots, v_n, v_{n+1} = v_1$. For consecutive vertices u, v, w in γ, we can replace v by some point $v' \in B_1(u) \cap B_1(w)$ by attaching the rhombus $[uvwv']$. We call this a rhombus equivalence. Then we prove the theorem directly for planar integral curves. Our approach is similar to ideas introduced in [GP22, §2].

Outline of the paper

We prove Theorem 1.3 in Section 2 because it is mostly self-contained. Then in Section 3 we introduce necessary notions to describe the moduli space of domes and curves. This is a generalization of many of the definitions and results given in [AK24] to allow for domes to bound unions of integral curves. Then we prove Theorem 1.4.3 in Section 4 with these techniques. Final remarks are given in Section 5.

Notation

As previously mentioned, $B_r(v)$ is the sphere of radius $r > 0$ around a point $v \in \mathbb{E}$, and for a list of points $v_1, \ldots, v_n \in \mathbb{E}$, let $[v_1 \ldots v_n]$ be the integral curve γ with vertices at the given points $v_1, \ldots, v_n, v_{n+1}$, where we use the convention that $v_{n+1} = v_1$ for an integral curve of length n throughout. For two points v, w, let (v, w) be the line containing the two points, let $[v, w]$ be the line segment connecting the two points, and let $|v, w|$ be the distance between the two points. For an integral curve γ, let $|\gamma|$ be the sum of all edge lengths of γ. Let $\mathcal{M}_n$ denote the set of all integral curves of length n. The set $\mathcal{M}_4$ is important in the proofs and is called the set of unit rhombi.

1.2 Every integral curve is cobordant to finitely many unit rhombi

In this section we prove Theorem 1.3, that every integral curve $\gamma \in \mathcal{M}_n$ is orientably cobordant to a finite union of rhombi $\rho_1 \cup \ldots \cup \rho_k$.

We say that two integral curves γ and η are *rhombus equivalent* if there exist finitely many unit rhombi $\rho_1, \ldots, \rho_k$ and a dome over $\gamma \cup \eta \cup \rho_1 \cup \ldots \cup \rho_k$. Here we say k is the number of *rhombi used* in the rhombus equivalence. This is similar to the definition of *flip equivalence*. (See e.g. [GP22, § 2.4].) We also want to distinguish when a rhombus equiv-

alence is orientable. However, when some of the integral curves share common edges, the resulting dome will not be purely 2-dimensional, so we define orientability carefully. For an integral curve γ, we call the surface formed by gluing the boundary of a disk to γ the *closure* of γ. We say a dome over $\gamma, \eta, \rho_1, \ldots, \rho_k$ is *orientable* if the dome, along with the closure of $\gamma, \eta, \rho_1, \ldots, \rho_k$ forms a closed, orientable surface. Clearly, if an integral curve γ is orientably rhombus equivalent to an integral curve which can be domed, then γ satisfies the existence condition of Theorem 1.3, and we can prove the theorem by keeping track of the number of rhombi used.

First, we show that every integral curve is orientably rhombus equivalent to a planar integral curve. An integral curve is *planar* if it lies in a plane $H \subset \mathbb{E}$.

Lemma 1.2.1. *Every integral curve γ is orientably rhombus equivalent to a planar integral curve. Moreover, for $|\gamma| = n$, it suffices to use $k = \binom{n}{2}$ rhombi.*

Proof. Choose two vertices v and w of γ, and take any plane H containing the line (v, w). This gives a decomposition of γ into two integral paths containing v and w, and we show that both can be made to lie entirely in H via rhombus equivalence.

Suppose η is an integral path with vertices $v = v_1, \ldots, v_m, v_{m+1} = w$. Let h_i denote the distance from v_i to the plane H, hence $h_1 = h_{m+1} = 0$. (See Figure 1.) Note that the heights h_i are all nonnegative, but the v_i may lie on different sides of H; this will not affect the proof. Choose v_i maximizing h_i. If the same height is achieved by multiple v_i, choose the one with the smallest index i. Note that this means $h_{i-1} < h_i \geq h_{i+1}$.

Consider the circle $B_1(v_{i-1}) \cap B_1(v_{i+1})$ which contains v_i. For each point $v_i' \in B_1(v_{i-1}) \cap B_1(v_{i+1})$, we can replace v_i by v_i' in η by rhombus equivalence via $[v_{i-1}v_iv_{i+1}v_i']$. (See Figure 2.) We can always choose v_i' to reduce h_i', the new distance from v_i' to H. (Eventually, we

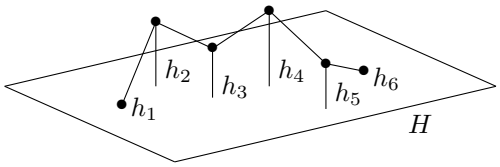

Figure 1.1: An integral path η above a plane H with heights h_i.

want to choose v_i' such that $h_i' = 0$ so that $v_i' \in H$ for every vertex. The following is an argument that we can always do this after at most $\binom{n}{2}$ rhombus equivalences.) Suppose we choose v_i' so that the line (v_{i-1}, v_i') is parallel to the line (v_i, v_{i+1}). (I.e., we choose v_i' so that the rhombus $[v_{i-1}v_iv_{i+1}v_i']$ is planar.) Then $h_i' = h_{i-1} + (h_{i+1} - h_i)$, and because $h_{i+1} \leq h_i$ we conclude that $h_i' \leq h_{i-1}$ for this choice of v_i'. To simplify our analysis of the number of rhombi used, suppose that we always choose v_i' so that $h_i' = h_{i-1}$

Note that either v_{i-1} or v_{i+1} may be on the other side of H relative to v_i, in which case the circle $B_1(v_{i-1}) \cap B_1(v_{i+1})$ will always intersect H. (If $B_1(v_{i-1}) \cap B_1(v_{i+1})$ did not intersect H, then h_i would not be a maximum height.) So in this case, we can always choose $v_i' \in H$.

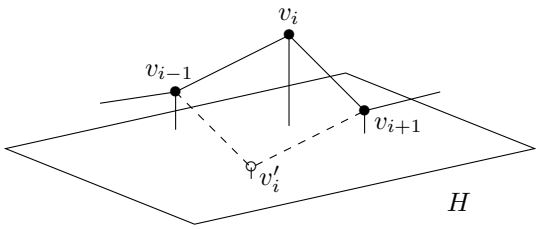

Figure 1.2: Adding a rhombus $[v_{i-1}v_iv_{i+1}v_i']$.

To count the number of rhombi used, view rhombus equivalence as an operation on the sequence $0, h_2, \ldots, h_m, 0$ of heights which takes the first maximum element h_i and replaces it with the smaller value of h_{i-1}. Suppose $\mathcal{H}$ is the set of all distinct heights achieved by the

original integral path η, and $\mathrm{wt} : \mathcal{H} \to \mathbb{Z}$ is a weight function which assigns a height h the number $\mathrm{wt}(h)$ of strictly smaller heights in $\mathcal{H}$. (I.e., the index of h when $\mathcal{H}$ is ordered smallest to largest, starting at index 0.) If η' is an integral path of length m such that every height h' is in $\mathcal{H}$, then we can define $\mathrm{wt}(\eta')$ as the sum $\mathrm{wt}(h'_1) + \ldots + \mathrm{wt}(h'_m)$ of weights of its heights. This weight is well defined on any integral path η' formed by applying rhombus equivalence to η, and after each application of rhombus equivalence the weight of the resulting integral path $\mathrm{wt}(\eta')$ decreases by at least 1. At the start, $\mathrm{wt}(\eta) \leq 0 + 1 + \ldots + (m-1) = \binom{m}{2}$, thus after $\binom{m}{2}$ rhombus equivalences, we will have an integral path of $\mathrm{wt}(\eta') = 0$, meaning it lies entirely in the plane H. And for the whole integral curve γ, we will need at most $\binom{m}{2} + \binom{n-m}{2} \leq \binom{n}{2}$ rhombi to find an integral curve which lies entirely in H.

To see that the rhombus equivalence is orientable, note that the closure of all the rhombi used in the rhombus equivalence is homeomorphic to an annulus. Thus the cobordism over γ, all of the rhombi used, and the resulting planar integral curve is orientable. □

We say that an integral curve $\gamma = [v_1 \ldots v_n]$ is *ϵ-packing around v_i* if for all j, the length $|v_i, v_j| < \epsilon$. In this case, we say that v_i is the *packing center* of γ, and when the packing center is understood we just say that γ is *ϵ-packing*. Next we prove that every planar integral curve is orientably rhombus equivalent to a 2-packing planar integral curve.

Lemma 1.2.2. *Every planar integral curve γ is orientably rhombus equivalent to a planar integral curve which is 2-packing around one of its vertices. Moreover, if $|\gamma| = n$, then it suffices to use $k = \binom{n}{2}$ rhombi.*

Proof. The existence of a rhombus equivalent 2-packing curve follows from the Steinitz Lemma, which can be stated as follows. (See e.g. [Bar08, Theorem 2.1].) For each dimension $d > 0$, there is a constant β_d such that for any unit vectors $u_1, \ldots, u_n \in \mathbb{R}^d$ satisfying $u_1 + \ldots + u_n = 0$, there is a permutation $\sigma \in S_n$ such that for each $1 \leq i \leq n$,

$$|u_{\sigma(1)} + \ldots + u_{\sigma(i)}| \leq \beta_d$$

For $d = 2$, Bergström showed the optimal value is $\beta_2 = \sqrt{5}/2$ in [Ber31]. However, we use the constant 2 because it is sufficient for the proof of Theorem 1.3 and gives clearer exposition.

Viewing the integral curve $\gamma = [v_1 \dots v_n]$ as a set of vectors $u_1, \dots, u_n$, with u_i pointing from v_i to v_{i+1}, we can swap a pair of consecutive vectors u_i and u_{i+1}. We add a rhombus containing the endpoints v_{i-1}, v_i, v_{i+1}, and the point v_i reflected across the line (v_{i-1}, v_{i+1}). This corresponds to the simple transposition $(i, i+1) \in S_n$. And because we can achieve any permutation $\sigma \in S_n$ by the product of simple transpositions, there exists a rhombus equivalent 2-packing planar integral curve around v_1. (See e.g. [Sta12].) Moreover, for every permutation $\sigma \in S_n$, the maximal length of σ in terms of simple transpositions is $\binom{n}{2}$, so this number of rhombi is sufficient.

Again, we see that this rhombus equivalence is orientable because the closure of all of the rhombi used in the rhombus equivalence is homeomorphic to an annulus. □

Now we prove the result of Theorem 1.3 for planar integral curves. Our proof is direct when $|\gamma| = 5$, and when $|\gamma| > 5$ we divide γ into pentagons.

Theorem 1.3. *Every integral curve γ is orientably cobordant to $\rho_1 \cup \dots \cup \rho_k$ for a finite set of unit rhombi $\rho_1, \dots, \rho_k \in \mathcal{M}_4$. Moreover, for $|\gamma| = n$, it suffices to take $k = n^2 + 2n - 12$ rhombi.*

Proof. From Lemma 1.2.1 and Lemma 1.2.2, we may assume without loss of generality that γ is planar and 2-packing around one of its vertices v_1. This uses $n(n-1)$ rhombi. Now we prove the statement for planar, 2-packing integral curves by dividing them into pentagons.

First, suppose γ is a pentagon $[v_1 \dots v_5]$. If the circumradius of the triangle $[v_1 v_3 v_4]$ is less than 1, then there is a point $z \in B_1(v_1) \cap B_1(v_3) \cap B_1(v_4)$. (See Figure 3, left.) Adding the

edges $[z, v_1]$, $[z, v_3]$ and $[z, v_4]$ gives a cobordism between γ and two unit rhombi $[v_1v_2v_3z]$ and $[v_1zv_4v_5]$. If the circumradius of the triangle $[v_1v_3v_4]$ is greater than 1, then we can perform a rhombus equivalence to construct a new integral curve γ' with the desired circumradius. Note that at most 3 rhombi are used.

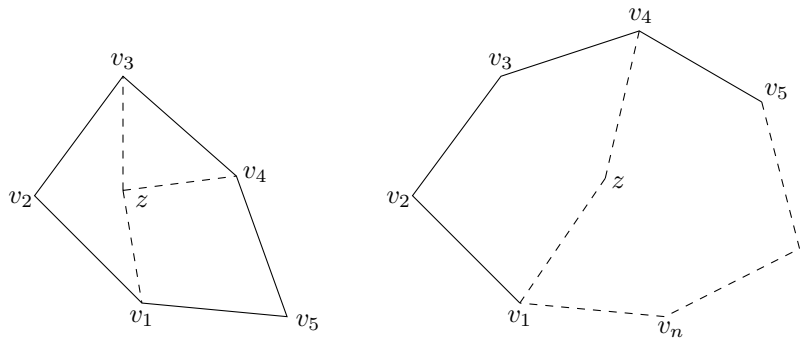

Figure 1.3: The $n = 5$ case and the general case.

In the general case, for a planar, 2-packing integral curve $\gamma = [v_1 \dots v_n]$ with $n > 5$, there is some point $z \in B_1(v_1) \cap B_1(v_4) \cap H$, where H is the plane containing γ. (See Figure 3, right.) We can divide γ into the planar pentagon $[v_1v_2v_3v_4z]$ and $\gamma' := [v_1zv_4 \dots v_n]$, which is a planar, 2-packing integral curve of length $n - 1$. Continuing this procedure divides γ into $n - 4$ pentagons, each of which use at most 3 rhombi. So in total at most $n(n-1) + 3(n-4) = n^2 + 2n - 12$ rhombi are used.

To see that this cobordism is orientable, note that when $n = 5$ the surface formed from the triangle and the closure of the rhombi used is homeomorphic to a disk. And in the general case, we just divide γ into the union of pentagons. □

1.3 Spaces of polygons and polyhedra

This section introduces definitions and proves technical results we need to prove Theorem 1.4.3, that not all integral curves are orientably cobordant to a unit rhombus. Our approach is inspired by techniques introduced by Anan'in and Korshunov, who gave an alternate proof of the negative answer to Kenyon's question for almost all integral curves in [AK24]. Specifically, we generalize Anan'in and Korshunov's results to graph surfaces with multiple boundary components corresponding to the union of multiple integral curves. We state our definitions here. For the original definitions and for a more detailed introduction, see [AK24, §2, §3].

A *sample polygon* is a finite 1-complex $P = (U, F)$ whose underlying space is homeomorphic to S^1. Here U is a set of vertices and $F = \{f_1, \ldots, f_k\}$ is a set of edges oriented and cyclically ordered with respect to the orientation of the circle. F is equipped with an edge length function $\ell : F \to \mathbb{R}_{>0}$ which satisfies a nondegeneracy condition $2\ell(f_i) < \ell(f_1) + \ldots + \ell(f_n)$ for all $1 \leq i \leq n$.

For a sample polygon P, the *space of polygons* $\mathbb{E}^P$ is the set of all continuous maps $p : P \to \mathbb{E}$ that are isometries on edges. That is, $\mathbb{E}^P$ is the set of all realizations of P in Euclidean space. Let $\mathrm{Isom}^+\mathbb{E}$ be the group of orientation preserving isometries of $\mathbb{E}$. The *moduli space of polygons* $\mathbb{E}^P/\mathrm{Isom}^+\mathbb{E}$ is the set of all realizations up to rigid motions. Let $\mathcal{E}$ be the subgroup of $\mathrm{Isom}^+\mathbb{E}$ of translations, and $SO(3)$ be the subgroup of rotations. Note that $\mathrm{Isom}^+\mathbb{E} \cong \mathcal{E} \rtimes SO(3)$. The *scheme of polygons* $\mathbb{E}^P/\mathcal{E}$ is the set of all realizations up to translations, but not rotations. Ultimately, we need to consider $\mathbb{E}^P/\mathrm{Isom}^+\mathbb{E}$, but in our proof we first consider $\mathbb{E}^P/\mathcal{E}$ and then quotient by the action of $SO(3)$.

For a vector of polygons $\mathbf{P} = (P_1, \ldots, P_n)$, let $\mathbb{E}^{\mathbf{P}}$ refer to the product $\mathbb{E}^{P_1} \times \ldots \times \mathbb{E}^{P_n}$.

Similarly, let $\mathbb{E}^{\mathbf{P}}/\mathrm{Isom}^+\mathbb{E}$ and $\mathbb{E}^{\mathbf{P}}/\mathcal{E}$ refer to the products $\mathbb{E}^{P_1}/\mathrm{Isom}^+\mathbb{E} \times \ldots \times \mathbb{E}^{P_n}/\mathrm{Isom}^+\mathbb{E}$ and $\mathbb{E}^{P_1}/\mathcal{E} \times \ldots \times \mathbb{E}^{P_n}/\mathcal{E}$, respectively. As an abuse of terminology, we still refer to these as the *space of polygons*, *moduli space of polygons* and *scheme of polygons* respectively. Note that the group of isometries always acts on each sample polygon separately, see § 1.5.1. To refer to the polygons explicity, we may write $\mathbb{E}^{P_1,\ldots,P_n}$ rather than $\mathbb{E}^{\mathbf{P}}$. (See Lemma 1.4.2.) We refer to the sets of edges as $F_1, \ldots, F_n$, individual edges as $f_j^i \in F_i$, and the edge length functions as $\ell_i : F_i \to \mathbb{R}_{>0}$.

As the name suggests, $\mathbb{E}^{\mathbf{P}}/\mathcal{E}$ is indeed a scheme. Note, however, that it may contain singular points. For one polygon, $p \in \mathbb{E}^P/\mathcal{E}$ is singular if and only if all $p(f_i)$ are parallel. For multiple polygons, $\mathbf{p} \in \mathbb{E}^{\mathbf{P}}/\mathcal{E}$ is singular if and only if some $p_i \in \mathbb{E}^{P_i}/\mathcal{E}$ is singular.

Lemma 1.3.1. *Let $\boldsymbol{p} \in \mathbb{E}^{\boldsymbol{P}}/\mathcal{E}$ be a singular point. Then $\dim T_{\boldsymbol{p}}(\mathbb{E}^{\boldsymbol{P}}/\mathcal{E}) = m + \dim(\mathbb{E}^{\boldsymbol{P}}/\mathcal{E})$, where m is the number of p_i which are singular in $\mathbb{E}^{P_i}/\mathcal{E}$.*

Proof. Since $\mathbb{E}^{\mathbf{P}}/\mathcal{E} = \mathbb{E}^{P_1}/\mathcal{E} \times \ldots \times \mathbb{E}^{P_n}/\mathcal{E}$, we have

$$\dim T_{\mathbf{p}}(\mathbb{E}^{\mathbf{P}}/\mathcal{E}) = \dim T_{p_1}(\mathbb{E}^{P_1}/\mathcal{E}) + \ldots + \dim T_{p_n}(\mathbb{E}^{P_n}/\mathcal{E}).$$

Now for a singular p_i, we have $\dim T_{p_i}(\mathbb{E}^{P_i}/\mathcal{E}) = 1 + \dim(\mathbb{E}^{P_i}/\mathcal{E})$ from [AK24, Lemma 3.2], else for a smooth p_i, we have $\dim T_{p_i}(\mathbb{E}^{P_i}/\mathcal{E}) = \dim(\mathbb{E}^{P_i}/\mathcal{E})$. Combining this for all p_i in $\mathbf{P}$ gives us the result. □

Consider the following explicit description of the scheme of polygons $\mathbb{E}^{\mathbf{P}}/\mathcal{E}$ for a list of polygons $\mathbf{P}$. A point $\mathbf{p} \in \mathbb{E}^{\mathbf{P}}/\mathcal{E}$ is a collection of maps $p_i : F_i \to \mathbb{E}$ which satisfy $\langle p_i(f_j^i), p_i(f_j^i)\rangle = \ell_i(f_j^i)^2$ for all i, j and $\sum_j p_i(f_j^i) = 0$ for all i. Similarly, for $\mathbf{p} \in \mathbb{E}^{\mathbf{P}}/\mathcal{E}$, a point $\mathbf{t}$ in the tangent space $T_{\mathbf{p}}(\mathbb{E}^{\mathbf{P}}/\mathcal{E})$ is a collection of maps $t_i : F_i \to \mathbb{E}$ satisfying $\langle t_i(f_j^i), p_i(f_j^i)\rangle = 0$ for all i, j and $\sum_j t_i(f_j^i) = 0$ for all i.

We generalize the definition of a graph surface given in [AK24] to allow for multiple boundary components as follows. A *genus n graph surface* S is a finite 2-dimensional simplicial complex with nondegenerate triangles and edges contained in a closed surface $\widehat{S}$ such that the complement $\mathcal{D} := \widehat{S} \smallsetminus S$ is homeomorphic to the disjoint union of n disks. This has the following data: a set of vertices V, a set of edges E with orientation, a set of triangles $\mathcal{T}$, and a map $\Phi : E \to E$ defined as $\Phi : e \mapsto -e$ which reverses orientation.

A graph surface of genus n has boundary $\partial\mathcal{D} = G_1 \cup \ldots \cup G_n$, where each G_i is a *boundary component* homeomorphic to S^1. Each boundary component G_i can be decomposed into the union $g_1^i \cup \ldots \cup g_{k_i}^i$ with a cyclic order of the edges $g_1^i, \ldots, g_{k_i}^i \in E$ such that g_j^i and g_{j+1}^i are consecutive for all i, j. Note that the list $g_1^i, \ldots, g_{k_i}^i$ admits repetitions with the same or opposite orientation. As an important special case, note that when a graph surface $S \subset \widehat{S}$ is contained in an orientable surface and contains no triangles, then every edge appears exactly twice, once with each orientation, in the boundary $\partial\mathcal{D}$. See [AK24, Remark 2.5], and note that each boundary component can be given the same orientation with respect to the oriented surface $\widehat{S}$.

Similarly, we generalize the definition of a *sample polyhedron* to allow for a genus n graph surface instead of just a genus 1 graph surface as in [AK24, Definition 2.1]. For us, a sample polyhedron will mean a genus n graph surface S equipped with an edge length function $\ell : \mathbb{E} \to \mathbb{R}_{>0}$ satisfying $\ell(e) = \ell(-e)$ for any edge $e \in E$ and $\ell(e_1) + \ell(e_2) > \ell(e_3)$ for any triangle $T \in \mathcal{T}$ with boundary $\partial T = e_1 + e_2 + e_3$. For a given sample polyhedron S, we also consider the *space of polyhedra* $\mathbb{E}^S$, the *moduli space of polyhedra* $\mathbb{E}^S/\mathrm{Isom}^+\mathbb{E}$ and the *scheme of polyhedra* $\mathbb{E}^S/\mathcal{E}$.

An explicit description for the scheme of polyhedra $\mathbb{E}^S/\mathcal{E}$ is given by the set of continuous maps $q : E \to \mathbb{E}$ satisfying

(i) $\langle q(e), q(e)\rangle = \ell(e)^2$ for all $e \in E$,

(ii) $q(-e) = -q(e)$ for all $e \in E$,

(iii) $q(e_1) + q(e_2) + q(e_3) = 0$ for all triangles $T \in \mathcal{T}$ with boundary $\partial T = e_1 + e_2 + e_3$,

(iv) for a set of generators $H \subset H_1(S, \mathbb{Z})$, $\sum_{e\in E} h_e q(e) = 0$ for any generator $\sum_{e\in E} h_e e \in H$.

Similarly, an explicit description for the tangent space $T_q(\mathbb{E}^S/\mathcal{E})$ is given by the set of continuous maps $s : E \to \mathbb{E}$ satisfying

(i') $\langle s(e), q(e)\rangle = 0$ for all $e \in E$,

and the previous conditions (ii) - (iv). See [AK24, §§2.7-9].

There is a boundary map which connects sample polyhedra and sample polygons. Let S be a sample polyhedron, with boundary components $G_1, \ldots, G_n$ where $G_i = g_1^i \cup \ldots \cup g_{k_i}^i$ in cyclic order. For each i, j, define an oriented edge f_j^i of length $\ell(g_j^i)$ and glue the edges $f_1^i, \ldots, f_{k_i}^i$ into a sample polygon P_i. We call the polygons $\mathbf{P}$ the *boundary polygons* of S. This defines a map $\delta : F_1 \cup \ldots \cup F_n \to E$ via $\delta : f_j^i \mapsto g_j^i$, and extends to a continuous map $\overline{\delta} : P_1 \cup \ldots \cup P_n \to S$. Thus $\overline{\delta}(f_j^i) = g_j^i$ for all i, j and $\overline{\delta}$ is an isometry on edges. Now $\overline{\delta}(P_i) = G_i$, and $\overline{\delta}(P_1 \cup \ldots \cup P_n) = \partial\mathcal{D}$. We call the map $\overline{\delta}$, or just δ, the *combinatorial boundary map* of the sample polyhedron S.

The boundary map induces a continuous map on schemes $\delta : \mathbb{E}^S/\mathcal{E} \to \mathbb{E}^{\mathbf{P}}/\mathcal{E}$ and a derivative map on the tangent spaces $d\delta : T_q(\mathbb{E}^S/\mathcal{E}) \to T_{q\circ\delta}(\mathbb{E}^{\mathbf{P}}/\mathcal{E})$ for any point $q : E \to \mathbb{E}$ in the scheme of polyhedra $\mathbb{E}^S/\mathcal{E}$. These maps are from precomposition with δ, see [AK24, §2.10].

Lastly, we define the collapse of a genus n graph surface S. Let $T \in \mathcal{T}$ be a triangle whose boundary ∂T contains a boundary edge g_j^i. We may collapse S at T. The resulting

simplicial complex $S' \subset \widehat{S}$ has the same vertices $V' = V$, one less pair of oriented edges $E' = E \smallsetminus \{g_j^i, -g_j^i\}$, and one less triangle $\mathcal{T}' = \mathcal{T} \smallsetminus \{T\}$. Note that S' is again a genus n graph surface. The boundary component G_i changes from $g_1^i \cup \ldots \cup g_j^i \cup \ldots \cup g_{k_i}^i$ to $g_1^i \cup \ldots \cup -e' \cup -e \cup \ldots \cup g_{k_i}^i$, where $\partial T = g_j^i + e + e'$. All other boundary components are unchanged. In terms of a realization $q : E \to \mathbb{E}$ in the scheme of polyhedra $\mathbb{E}^S/\mathcal{E}$, collapse corresponds to restriction.

Lemma 1.3.2. *Let S' be a sample polyhedra obtained from S by collapse of a triangle, and let $q : E \to \mathbb{E}$ be a realization in the scheme of polyhedra $\mathbb{E}^S/\mathcal{E}$. Denote by $q' = q|_{E'} : E' \to E$ the restriction of q to E'. Then $q' \in \mathbb{E}^{S'}/\mathcal{E}$. Similarly, for $s : E \to \mathbb{E}$ in $T_q(\mathbb{E}^S/\mathcal{E})$, denote by $s' = s|_{E'} : E' \to \mathbb{E}$ the restriction of s to E'. Then $s' \in T_{q'}(\mathbb{E}^{S'}/\mathcal{E})$.*

Proof. This is exactly the statement of [AK24, Proposition 4.2 (i)]. The same proof follows exactly when we allow for a genus n graph surface. □

Consider the group $SO(3)^{\times n}$ acting on $\mathbb{E}^{\mathbf{P}}/\mathcal{E}$, where each copy of $SO(3)$ acts on the corresponding scheme of polygons $\mathbb{E}^{P_i}/\mathcal{E}$. For $\mathbf{p} \in \mathbb{E}^{\mathbf{P}}/\mathcal{E}$, we need to describe the tangent space $T_{\mathbf{p}}SO(3)^{\times n}\mathbf{p}$. Recall the Lie algebra $\mathfrak{so}_3$ of the Lie group $SO(3)$ with the following description.

$$\mathfrak{so}_3 = \{a \in \mathrm{Hom}_{\mathbb{R}}(\mathbb{E}, \mathbb{E}) \mid \langle a(e), e' \rangle + \langle e, a(e') \rangle = 0 \ \forall e, e' \in E\}.$$

Let $\mathfrak{so}_3^{\times n}$ be the set of vectors $\mathbf{a} = (a_1, \ldots, a_n)$, where each $a_i \in \mathfrak{so}_3$. We have the following description of the tangent space to the $SO(3)^{\times n}$ orbit on $\mathbb{E}^{\mathbf{P}}/\mathcal{E}$.

Lemma 1.3.3. *Let $\boldsymbol{p} \in \mathbb{E}^{\boldsymbol{P}}/\mathcal{E}$. The tangent space $T_{\boldsymbol{p}}SO(3)^{\times n}\boldsymbol{p}$ to the $SO(3)^{\times n}$-orbit of $\boldsymbol{p}$ is given by*

$$\begin{aligned} T_{\boldsymbol{p}}SO(3)^{\times n}\boldsymbol{p} &= T_{p_1}SO(3)p_1 \times \ldots \times T_{p_n}SO(3)p_n \\ &= \{\boldsymbol{a} \circ \boldsymbol{p} = \{a_i \circ p_i : F_i \to \mathbb{E}\} \mid \boldsymbol{a} \in \mathfrak{so}_3^{\times n}\}. \end{aligned}$$

Proof. The first line is immediate because each copy of $SO(3)$ acts independently on each copy of $\mathbb{E}^{P_i}/\mathcal{E}$. Then for a single $SO(3)$ acting on $p_i \in \mathbb{E}^{P_i}/\mathcal{E}$, we know $T_{p_i}SO(3)p_i = \{a_i \circ p_i : F_i \to \mathbb{E} \mid a_i \in \mathfrak{so}_3\}$ from [AK24, §3.1]. □

The final ingredient is a symplectic form on the scheme of polygons $\mathbb{E}^{\mathbf{P}}/\mathcal{E}$. Consider the skew symmetric form ω given by the formula

$$\omega_{\mathbf{p}}(\mathbf{t}, \mathbf{t'}) := \sum_{i=1}^{n} \sum_{j=1}^{k_i} \frac{t_i(f_j^i) \wedge t_i'(f_j^i) \wedge p_i(f_j^i)}{\ell_i(f_j^i)^2 \nu} = \sum_{i=1}^{n} \omega_{p_i}(t_i, t_i').$$

Here ν is the volume form on $\mathbb{E}$, and $\mathbf{t}, \mathbf{t'} \in T_{\mathbf{p}}(\mathbb{E}^{\mathbf{P}}/\mathcal{E})$. ω_{p_i} refers to the sum containing all components of P_i, and corresponds to [AK24, §3.3, Formula V]. We show that the kernel of this form is exactly the tangent space to the $SO(3)^{\times n}$ orbit of a point $\mathbf{p} \in \mathbb{E}^{\mathbf{P}}/\mathcal{E}$, so that $\omega_{\mathbf{p}}$ descends to the moduli space of polygons $\mathbb{E}^{\mathbf{P}}/\mathrm{Isom}^+\mathbb{E}$. Note that by kernel we are considering $\omega_{\mathbf{p}}$ as a map $T_{\mathbf{p}}(\mathbb{E}^{\mathbf{P}}/\mathcal{E}) \to T_{\mathbf{p}}(\mathbb{E}^{\mathbf{P}}/\mathcal{E})^*$. That is, the kernel is the set of points $\mathbf{t} \in T_{\mathbf{p}}(\mathbb{E}^{\mathbf{P}}/\mathcal{E})$ such that for all $\mathbf{t'} \in T_{\mathbf{p}}(\mathbb{E}^{\mathbf{P}}/\mathcal{E})$, we have $\omega_{\mathbf{p}}(\mathbf{t}, \mathbf{t'}) = 0$. For more background on the symplectic structure of the moduli space of polygons, see [KM96] and [Kly96].

Lemma 1.3.4. *The tangent space $T_{\boldsymbol{p}}(SO(3)^{\times n}\boldsymbol{p})$ to the $SO(3)^{\times n}$ orbit of any point $\boldsymbol{p} \in \mathbb{E}^{\boldsymbol{P}}/\mathcal{E}$ coincides with the kernel of the form $\omega_{\boldsymbol{p}}$ on $T_{\boldsymbol{p}}(\mathbb{E}^{\boldsymbol{P}}/\mathcal{E})$.*

Proof. For a single $p_i \in \mathbb{E}^{P_i}/\mathcal{E}$, we know the kernel of the form ω_{p_i} on $T_{p_i}(\mathbb{E}^{P_i}/\mathcal{E})$ corresponds to $T_{p_i}SO(3)p_i$ from [AK24, Lemma 3.4]. This immediately shows that $T_{\mathbf{p}}SO(3)^{\times n}\mathbf{p} \subset \ker \omega_{\mathbf{p}}$, as each term in the sum will be 0. For the reverse inclusion, we repeat the dimension counting argument from [AK24, Lemma 3.4] with our Lemma 1.3.1 in place of Lemma [AK24, Lemma 3.2]. This shows the spaces have the same dimension, so they are equal. □

1.4 Not every integral curve is cobordant to a unit rhombus

This section proves that not every integral curve is orientably cobordant to a unit rhombus. Our method is to generalize [AK24, Theorem 4.3] to allow for graph surfaces of arbitrary

genus. We rephrase a cobordism of a certain combinatorial type as a sample polyhedron with multiple boundary components, and project down to the smaller moduli space with one fewer boundary component to account for any possible unit rhombus to be chosen for the cobordism.

Theorem 1.4.1. *Let $S \subset \widehat{S}$ be a genus n graph surface, with boundary polygons $\boldsymbol{P}$, where $\widehat{S}$ is a closed orientable surface. Then*

$$\delta : \mathbb{E}^S / Isom^+\mathbb{E} \to \mathbb{E}^{\boldsymbol{P}} / Isom^+\mathbb{E},$$

is isotropic. In particular, the rank of $d\delta$ is at most half the dimension of the moduli space of polygons.

Note that the skew symmetric form on $\mathbb{E}^{\mathbf{P}}/\mathrm{Isom}^+\mathbb{E}$ is induced by the skew symmetric form ω on $\mathbb{E}^{\mathbf{P}}/\mathcal{E}$ after taking the quotient by the action of $SO(3)^{\times n}$. We show that the pullback of this skew symmetric form ω' is null. Also note that the orientability hypothesis is necessary here, see § 1.5.3

Proof. The proof of [AK24, Theorem 4.3] follows word for word to show that $\delta : \mathbb{E}^S/\mathcal{E} \to \mathbb{E}^{\mathbf{P}}/\mathcal{E}$ is isotropic by a series of collapses. To show that this survives in the quotient by $SO(3)^{\times n}$, we use Lemma 1.3.4. Because $T_{\mathbf{p}} SO(3)^{\times n}\mathbf{p} = \ker \omega_{\mathbf{p}}$, taking the quotient by $SO(3)^{\times n}$ on $\mathbb{E}^{\mathbf{P}}/\mathcal{E}$ gives a new nondegenerate skew-symmetric form ω' on $\mathbb{E}^{\mathbf{P}}/\mathrm{Isom}^+\mathbb{E}$, and the pullback of the form to $\mathbb{E}^S/\mathrm{Isom}^+\mathbb{E}$ is still null. □

Now we can phrase the condition of being cobordant in terms of a sample polyhedron with multiple boundary components.

Lemma 1.4.2. *Let $S \subset \widehat{S}$ be a sample polyhedron with boundary polygons $P_1, P_2, P_3 \in \mathcal{M}_n$, where $\widehat{S}$ is an orientable closed surface. Let π be the projection from $\mathbb{E}^{P_1,P_2,P_3}/Isom^+\mathbb{E} \to \mathbb{E}^{P_1,P_2}/Isom^+\mathbb{E}$. Then $\pi \circ \delta(\mathbb{E}^S/Isom^+\mathbb{E}) \subset \mathbb{E}^{P_1,P_2}/Isom^+\mathbb{E}$ has measure 0.*

Proof. Take the reduction of the scheme $\mathbb{E}^S/\mathrm{Isom}^+\mathbb{E}$ because we are only interested in the set theoretical image of the space of polyhedra up to sets of measure 0. Consider its smooth locus which is open and of full measure. Now δ is a smooth map of smooth manifolds, and by Theorem 1.4.1 the rank of its differential is at most half the dimension of the target manifold. Let $\dim \mathbb{E}^{P_i}/\mathrm{Isom}^+\mathbb{E} = m$. Then $\dim \mathbb{E}^{P_1,P_2,P_3}/\mathrm{Isom}^+\mathbb{E} = 3m$, so $d\delta$ has rank $\leq \frac{3}{2}m$. But $\dim \mathbb{E}^{P_1,P_2}/\mathrm{Isom}^+\mathbb{E} = 2m$, and so the map $d\pi \circ d\delta$ has rank $\leq \frac{3}{2}m < 2m$. By Sard's theorem, the image $\pi \circ \delta(\mathbb{E}^S/\mathrm{Isom}^+\mathbb{E})$ has measure 0 in $\mathbb{E}^{P_1,P_2}/\mathrm{Isom}^+\mathbb{E}$. □

We prove the main result of the section by showing that in general we cannot find a cobordism from two unit rhombi down to one unit rhombus.

Theorem 1.4.3. *The set of unit rhombi $\rho_1, \rho_2 \in \mathcal{M}_4$ such that $\rho_1 \cup \rho_2$ is orientably cobordant to a third unit rhombus $\rho_3 \in \mathcal{M}_4$ has measure* 0.

Proof. Any dome that forms a cobordism between two unit rhombi $\rho_1, \rho_2 \in \mathcal{M}_4$ and another unit rhombus $\rho_3 \in \mathcal{M}_4$ is exactly a genus 3 graph surface S whose boundary $\delta(\mathbb{E}^S/\mathrm{Isom}^+\mathbb{E}) \subset \mathbb{E}^{\rho_1,\rho_2,\rho_3}/\mathrm{Isom}^+\mathbb{E}$. Since we can take any unit rhombus ρ_3, we care about the projection $\pi \circ \delta(\mathbb{E}^S/\mathrm{Isom}^+\mathbb{E}) \subset \mathbb{E}^{\rho_1,\rho_2}/\mathrm{Isom}^+\mathbb{E}$. This has measure 0 from Lemma 1.4.2, and there are only countably many domes, so we conclude that the set of pairs of rhombi $\rho_1, \rho_2 \in \mathcal{M}_4$ such that $\rho_1 \cup \rho_2$ is cobordant to a third unit rhombus $\rho_3 \in \mathcal{M}_4$ has measure 0. □

Glazyrin and Pak did not consider unions of integral curves, so Theorem 1.4.3 is not an answer to Conjecture 1.1.1 in the orientable case, but we give one in the following.

Theorem 1.2. *There exists an integral curve γ of length* 5 *that is not orientably cobordant to any unit rhombus ρ.*

Proof. Choose a pair of unit rhombi $\rho, \rho' \in \mathcal{M}_4$ such that $\rho \cup \rho'$ is not cobordant to any third unit rhombus $\rho'' \in \mathcal{M}_4$. Let $\rho = [v_1v_2v_3v_4]$ and $\rho' = [v_1'v_2'v_3'v_4']$. Position ρ and ρ' so that $v_1 = v_1'$, $v_2 = v_2'$, and the distance $|v_3, v_3'| = 1$. Note that from our definition of $\mathbb{E}^{\rho,\rho'}/\mathrm{Isom}^+\mathbb{E}$,

it does not matter how ρ and ρ' are oriented relative to each other, see §1.5.1. By adding the unit triangle $[v_2, v_3, v_3']$, we see that $\rho \cup \rho'$ is cobordant to the perimeter $\gamma = [v_1 v_4 v_3 v_3' v_4']$. Therefore, our choice of ρ, ρ' implies that γ is not cobordant to any unit rhombus, and γ has only one connected component. □

Glazyrin and Pak conjectured that a positive answer to Conjecture 1.1.1 would involve showing a cobordism between an integral curve and finitely many unit rhombi, and then a cobordism between two unit rhombi and one unit rhombus, see [GP22, Conj. 5.15, Conj. 5.16]. Thus Theorem 1.4.3 is a negative answer to [GP22, Conj. 5.16] and Theorem 1.2 is a negative answer to Conjecture 1.1.1, both in the orientable case.

1.5 Final remarks

1.5.1 Relative orientation of integral curves

The proof of Theorem 1.4.3 does not account for the fact that the unit rhombi in question can be oriented in some manner with respect to each other. That is, we have chosen to define $\mathbb{E}^{\mathbf{P}}/\mathrm{Isom}^+\mathbb{E}$ with the group of orientation preserving isometries $\mathrm{Isom}^+\mathbb{E}$ acting on each polygon separately. However, we could consider $\mathrm{Isom}^+\mathbb{E}$ as acting on all of the spaces together, so instead of $\mathbb{E}^{P_1}/\mathrm{Isom}^+\mathbb{E} \times \ldots \times \mathbb{E}^{P_n}/\mathrm{Isom}^+\mathbb{E}$ we would consider $\mathbb{E}^{P_1}/\mathrm{Isom}^+\mathbb{E} \times \mathbb{E}^{P_2} \times \ldots \times \mathbb{E}^{P_n}$. This approach could answer more general questions. For example, Glazyrin and Pak conjectured that there are two unit triangles $\Delta_1, \Delta_2 \subset \mathbb{E}$ which are not cobordant, see [GP22, Conjecture 5.13]. In this question, the relative translation and rotation of the triangles is important, so our current techniques are insufficient.

Additionally, consider Steinhaus' 1957 problem on tetrahedral chains, see [Stei57]. A tetrahedral chain is a polyhedron constructed by attaching regular tetrahedra along faces to form a chain. These can be viewed as cobordisms between two triangles that satisfy stricter

conditions than general domes. Steinhaus asked if tetrahedral chains can be closed, and if they are dense in $\mathbb{E}$. In contrast to general domes, the first question was shown to be false by Swierczkowski in [Świ59]. However, the second question remains open. Recently, Stewart showed in [Stew19] that the group generated by reflections across the faces of a regular tetrahedra is dense in $SO(3)$, but this does not resolve Steinhaus' question because it does not consider the translations in the full group $SO(3) \rtimes \mathbb{E}$. I.e., Stewart's approach considers only the relative rotation, not the relative translation of the two triangles.

1.5.2 Asymptotics of the number of rhombi required in Theorem 1.3

The minimal number k of unit rhombi needed for the cobordism in Theorem 1.3 gives a measure of complexity for an integral curve γ. In contrast to Conjecture 1.1.1 which proposed that $k = 1$ for all γ, we conjecture that $k = \Theta(|\gamma|)$. Theorem 1.3 gives a quadratic upper bound $k = O(|\gamma|^2)$. We do not believe this is optimal. For instance, the proofs of Lemma 1.2.1, Lemma 1.2.2 do not use any triangles in the rhombus equivalences; only rhombi are added. And the proofs could be optimized to improve the coefficients of the bound, for instance, by choosing three points in the plane H rather than two in the proof of Lemma 1.2.1, but this would still give a quadratic bound in $|\gamma|$. Additionally, Pak proposes a modified proof of Theorem 1.3 which uses a reduction to generic integral curves rather than planar integral curves to improve to a linear bound.[1] (See [GP22, §2] for terminology.) We also conjecture that the construction in Theorem 1.4.3 can be extended to arbitrarily many rhombi to prove that $k = \Omega(|\gamma|)$.

1.5.3 Orientability is necessary in Theorem 1.4.1

The orientability hypothesis in Theorem 1.4.1 is necessary for the cancellation argument, see [AK24, Remark 2.3] for more detail, and [AK24, Remark 4.4] for a counterexample with a

[1] I. Pak, Personal communication.

non-orientable surface. This limits the techniques used in this paper to the orientable case, and new techniques may be necessary to study non-orientable cobordisms.

CHAPTER 2

Universality of polyhedral linkages

2.1 Introduction

A planar linkage is a straight line realization of a graph in $\mathbb{R}^2$ where each edge is required to have a specified length. One may also fix some vertices to be realized at a specific point in $\mathbb{R}^2$, thus constraining the possible realizations of the other vertices. Planar linkages can be used to "compute" functions in the following sense. Suppose $U \subset \mathbb{R}^2$ is an open set and $F : U \to \mathbb{R}^2$ is a function. We say that a planar linkage *defines* F on the neighborhood U if the linkage has an input vertex x and an output vertex y, such that whenever x is realized in U, then y is constrained to be realized at $F(x)$. In this case, we say the linkage is *functional*. (See e.g. [DO05], [Pak09].)

Famously, planar linkages are universal in the sense that they can realize any polynomial function in any bounded region. This result is known as Kempe's Universality Theorem after Kempe's 1875 paper [Kem75]. (See a generalization in modern terminology in [KM02].) Alternatively, we may fix the output vertex to a specific point, which constrains the input vertex to realize or "trace" the zero locus of the defined function. Such linkages are called *closed*. In this setting, planar linkages can realize any bounded region of an algebraic set, or as popularized by Thurston, they can "sign your name". (See [King99] for a historical account.)

We say that a planar linkage is *embedded* if its edges do not cross and its vertices are distinct. Kempe's original proof did not consider embedding, and critically relied on linkages

which are not planar graphs. Nevertheless, Kempe's Universality Theorem was proved with an embedded construction in [AD+16], settling a question of Shimamoto from 2004.

In this paper, we prove a version of Kempe's Universality Theorem that holds for embedded linkages in dimension three and generalizes to higher dimensions. We consider *polyhedral linkages*, which replace the straight line graphs in $\mathbb{R}^2$ used in planar linkages with polyhedral complexes of codimension one satisfying certain properties. The term polyhedral linkage was first coined by Goldberg in [Gol42]. In three dimensions, polyhedral linkages are closely related to notions of *rigid origami*, but in this case our surface may have any topology. (See [DO05], [GZ19].) Our definition is modeled after the definition of planar linkages given by Kapovich and Millson in [KM02]. (See § 2.2.) We note versions of Kempe's Universality Theorem have previously been proven for graphs embedded in $\mathbb{R}^n$ by [King98] and [Abb08]. A polyhedral linkage can be converted to a graph linkage by taking the vertex set and defining a clique on each codimension one complex. Our new contribution is that these polyhedral linkages can be embedded, extending the work of [AD+16] to three dimensions and higher.

Theorem 2.1.1. *Let $U \subset \mathbb{R}^3$ be a bounded, open set, and $F : U \to \mathbb{R}^3$ be a polynomial function. There exists an embedded, functional polyhedral linkage $\mathcal{P}$ which defines F on U. Moreover, this construction generalizes to all higher dimensions.*

We also generalize the corollary of Kempe's Universality Theorem for closed linkages. That is, to use Thurston's phrasing, there exist embedded polyhedral linkages which can "sign" any algebraic set in $\mathbb{R}^3$.

Corollary 2.1.2. *Let $U \subset \mathbb{R}^3$ be a bounded, open set, and $S \subset \mathbb{R}^3$ be an algebraic set. Then there is an embedded polyhedral linkage which realizes $S \cap U$. Moreover, this construction generalizes to all higher dimensions.*

Kempe's Universality Theorem extends to a stronger result that for every choice of constants $m_1, m_2 \geq 1$, each polynomial function $F : (\mathbb{R}^2)^{m_1} \to (\mathbb{R}^2)^{m_2}$ can be realized by planar

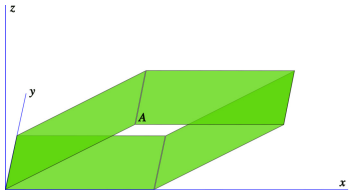

Figure 2.1: A polyhedral linkage.

linkages on an open bounded set. (See [KM02].) However, allowing multiple inputs and outputs poses a separate problem for embedded linkages. For example, consider a function with two inputs. If this were simulated by a physical machine, then the two input vertices may be realized at the same point. This would mean that the physical mechanisms should be able to 'pass through each other'. A similar problem can occur with output vertices.

To address this problem, we propose a modification to the definition of a functional linkage which considers each input and output vertex relative to its own reference coordinate frame. Specifically, in the forgetful maps defining the input and output vertices, we introduce a postcomposition which translates each coordinate. (See §2.2, and [KM02] for comparison.) This allows us to extend the vector version of Kempe's Universality Theorem to three dimensions and above with embedded linkages.

Our construction of functional polyhedral linkages centers around an efficient way to generate linear motion in three dimensions. In $\mathbb{R}^2$, finding a linkage which produces linear motion was a fundamental problem in the field. (For a history of the solution, see [KM02], §14.) However, the construction in $\mathbb{R}^3$ is comparatively simpler. In fact, in our current terminology a polyhedral linkage which achieves linear motion was first discovered by Sarrus in 1853, several years before any solution in $\mathbb{R}^2$ has been published. (See [Sar53], [Gol42] and also [WKA16]) Our construction is based on Sarrus' linkage with modifications to create a periodic flexing. Specifically, for any $0 < a < b$, we produce an embedded polyhedral linkage whose length in one dimension varies continuously in the interval (a, b), and which is arbitrarily small in all other dimensions. (See § 2.3.)

We set up an array of these *extender* linkages arranged parallel to each other in a fixed plane. The length of each extender encodes a scalar value, and the register of extenders allows us to encode a vector value. Note that this differs fundamentally from registers used in digital computers because each extender stores a value with infinite precision, but the range of values an extender can hold is still limited by its construction, i.e., by the chosen values of a and b. (See § 2.4.)

Computations are decomposed into a sequence of elementary operations. Each elementary operation uses an input register and an output register, which is a parallel translate of the input register. The output of the operation is stored in an extender in the output register by attaching both the output extender, and all input extenders, to a specific elementary linkage. (See § 2.4) These are generalizations of elementary planar linkages, in particular the pantograph and Peaucellier inversor, to higher dimensions, sometimes with slight modifications so that they are embedded. (See §2.2 and [KM02] §6 for comparison.) All other values in the original register are faithfully copied to the output register by rigid linkages.

We prove our main results, Theorem 2.1.1 and Corollary 2.1.2, by showing that all polynomial functions can be decomposed into elementary operations which can be performed by polyhedral linkages. Then we construct a polyhedral linkage in $\mathbb{R}^3$ which has a point that can be moved freely in a 3-dimensional region, and which records the coordinates of this point in a register of 3 extenders. (See § 2.5.) We use this register as the beginning of our computation, and attach a similar linkage to combine the final output register into the coordinates of a single output vertex. The generalization to multiple inputs and outputs is simple with our convention of separate reference frames. (See § 2.2.) The general case in higher dimensions is then immediate by extruding our construction. (See § 2.6.1.)

2.2 Polyhedral linkages

Here we give a general definition of a polyhedral linkage in two dimensions or higher. All of the constructions take place in two or three dimensions, and generalizations to higher dimensions are immediate. Our definition is a direct generalization of the definition of a planar linkage to include a codimension 1 polyhedral complex realized in $\mathbb{R}^n$. See [KM02] for motivation and a full definition for planar linkages.

Let $\mathcal{P}$ be a polyhedral complex in $\mathbb{R}^n$. We say that $\mathcal{P}$ is *pure* if every maximal polytope has the same dimension, and we say that $\mathcal{P}$ is *proper* if the intersection of any two k-dimensional faces in $\mathcal{P}$ is either $\varnothing$, or a $(k-1)$-dimensional face in $\mathcal{P}$. A straight line graph with fixed edge lengths is exactly a 1-dimensional pure, proper polyhedral complex in $\mathbb{R}^2$.

A *polyhedral linkage* of dimension n is a pair $(\mathcal{P}, W)$, where $\mathcal{P}$ is a n-dimensional pure, proper polyhedral complex in $\mathbb{R}^{n+1}$, and $W \subset \mathcal{V}(\mathcal{P})$ is a subset of the vertices of $\mathcal{P}$ called the *fixed vertices*. When clear by context, we will refer to the polyhedral linkage as $\mathcal{P}$ without reference to W.

A *realization* of $\mathcal{P}$ is a map $\phi : \mathcal{V}(\mathcal{P}) \to \mathbb{R}^{n+1}$ such that for each maximal face $F \in \mathcal{P}$, the vertices $\{\phi(v) \mid v \in F \cap \mathcal{V}(\mathcal{P})\}$ form the vertices of a polytope congruent to F. I.e., the maximal polytopes can be rearranged by individual rigid motions as long as they all fit together in the same structure. The $(n-1)$-dimensional faces act as "joints", allowing the structure to flex or hinge. The set of all realization, $C(\mathcal{P})$, is called the *configuration space* of $\mathcal{P}$.

Given a set of points Z in $\mathbb{R}^{n+1}$ and a bijection $f : W \to Z$, a realization $\phi : \mathcal{V}(\mathcal{P}) \to \mathbb{R}^{n+1}$ is said to be *relative to* f if $\phi(w) = f(w)$ for each $w \in W$. The set of all relative realizations to f, $C(\mathcal{P}, f)$, is called the *relative configuration space*.

We say that a realization $\phi \in C(\mathcal{P}, f)$ is *embedded* if the interiors of all maximal faces are pairwise disjoint. The set of all embedded realizations, $C^e(\mathcal{P}, f)$, forms an open subset

of $C(\mathcal{P}, f)$.

For example, consider the 2-dimensional polyhedral linkage $\mathcal{P}$ formed by removing two opposite faces of a cube. Let W be the vertices of one of the remaining faces of the cube, let Z be the four points $\{(0,0,0),(1,0,0),(1,1,0),(0,1,0)\}$ in the xy-plane, and f assigning W to Z in cyclic order. (See Figure 2.1.) The relative configuration space $C(\mathcal{P}, f)$ consists of three intersecting smooth curves and is naturally identified with the moduli space of the square, [KM02], §3. However, the embedded realization space $C^e(\mathcal{P}, f)$ is identified with the set $\{x^2 + y^2 = \ 1; z \ \neq \ 0\}$, where the location of the vertex A determines the entire configuration when A is not on the xy-plane. The points where A is on the xy-plane correspond to self-intersecting realizations of $\mathcal{P}$, and are included in the other two curves in $C(\mathcal{P}, f)$. Any physical model which is built to emulate the behavior of $\mathcal{P}$ can naturally move within a single connected component of $C^e(\mathcal{P}, f)$.

Next we formally define *functional linkages*. Let $m_1, m_2 \geq 1$ and let

$$F : \mathbb{R}^{(n+1)m_1} \longrightarrow \mathbb{R}^{(n+1)m_2}$$

be a given function. A *functional linkage* is a polyhedral linkage $\mathcal{P}$ of dimension n with two distinguished sets of vertices $\{I_1, \ldots, I_{m_1}\}$ called *input vertices* and $\{O_1, \ldots, O_{m_2}\}$ called *output vertices*. We also define two forgetful maps $p : C(\mathcal{P}, f) \to \mathbb{R}^{(n+1)m_1}$ and $q : C(\mathcal{P}, f) \to \mathbb{R}^{(n+1)m_2}$ as

$$p(\phi) = (\phi(I_1) + X_1, \ldots, \phi(I_{m_1}) + X_{m_1}),$$

$$q(\phi) = (\phi(O_1) + Y_1, \ldots, \phi(O_{m_2}) + Y_{m_2}),$$

for some choice of translations $X_1, \ldots, X_{m_1}, Y_1, \ldots, Y_{m_2} \in \mathbb{R}^{n+1}$. We say that $\mathcal{P}$ *defines* the function F at a point $\mathcal{O} \in \mathbb{R}^{(n+1)m_1}$ if there is a commutative diagram

$$\begin{array}{ccc} & C(\mathcal{P}, f) & \\ {\scriptstyle p}\swarrow & & \searrow{\scriptstyle q} \\ \mathbb{R}^{(n+1)m_1} & \xrightarrow{\quad F \quad} & \mathbb{R}^{(n+1)m_2} \end{array}$$

and p is a regular topological branched cover of a bounded open set $U \subset \mathbb{R}^{(n+1)m_1}$ containing the point $\mathcal{O}$. Alternatively, we say that $\mathcal{P}$ is a *functional linkage* for the germ $(F, \mathcal{O})$. Moreover, we say that a functional linkage $\mathcal{P}$ is *embedded* if there exists a connected component $E \subset C^e(\mathcal{P}, f)$ such that the restrictions $p|_E, q|_E$ still form a commutative diagram.

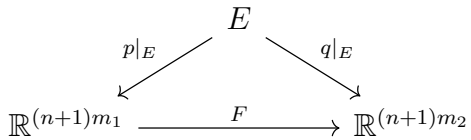

Finally, we say that a functional linkage $\mathcal{P}$ is *closed* if the output vertices are also fixed vertices. In this case, the image of the input map corresponds to the zero set of the defined function, and we say the $\mathcal{P}$ *realizes* U, where $U := p(C(\mathcal{P}, f))$, or $U := p|_E(E)$ in the embedded case.

2.3 Linear motion in three dimensions

In this section we give a construction which is a modification of Sarrus' linkage for linear motion. We construct an infinite linkage, periodic under translation, which flexes linearly and remains periodic during flexion, while the length of the periodicity vector changes in length but not direction. Moreover, any finite sublinkage which consists of a whole number of periods retains this property wherever periodicity is well defined. This is important for scalability in the construction of embedded polyhedral linkages.

Consider the planar linkage shown in Figure 2.2. The vertices A and B are fixed at $(0, 0)$ and $(1, 0)$, respectively. All other vertices are allowed to move freely, and all edges have length 1.

The vertex E may move within the 2-dimensional region $\{x^2 + y^2 \leq 4\}$. Suppose we replace each edge of this linkage with a 2-dimensional complex by taking the product with the unit interval. See Figure 2.3. We call this operation *extrusion*. In this case, we *extrude*

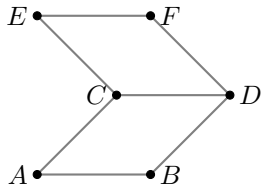

Figure 2.2: A planar linkage which achieves a 2-dimensional range of motion.

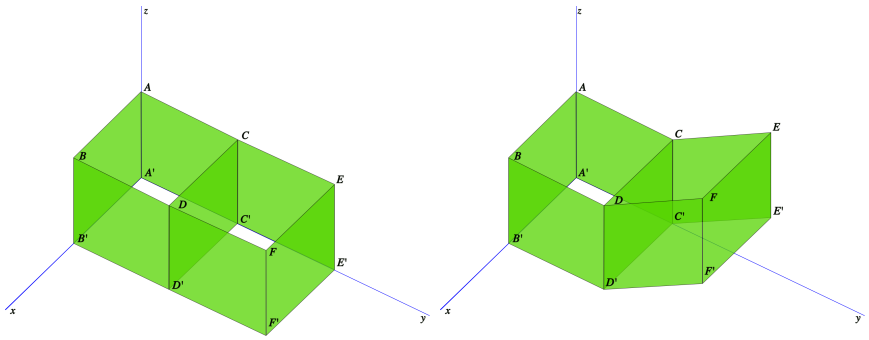

Figure 2.3: A polyhedral linkage which achieves a 2-dimensional range of motion.

a planar linkage to a polyhedral linkage, and in general, we may extrude a n-dimensional polyhedral linkage to a $(n+1)$-dimensional polyhedral linkage. In this case, the vertices corresponding to E in the extruded polyhedral linkage in Figure 2.3, namely E and E', still move within a 2-dimensional region. They do not gain an extra dimension of flexibility.

The linkage is made relative by fixing the vertices A, B, A' and B' to be at $(0,0,1), (1,0,1), (0,0,0)$ and $(1,0,0)$, respectively. All other vertices are allowed to move freely, and all edges have length 1.

The vertex E may move within the region $\{x^2 + y^2 \leq 4; z = 1\}$, which is still 2-dimensional. (E' moves in the translate of this region to $z = 0$.) We further constrain this linkage to restrict the motion to be 1-dimensional. We add two vertices, X and Y, which form two rectangles $ABYX$ and $EFYX$. See Figure 2.4.

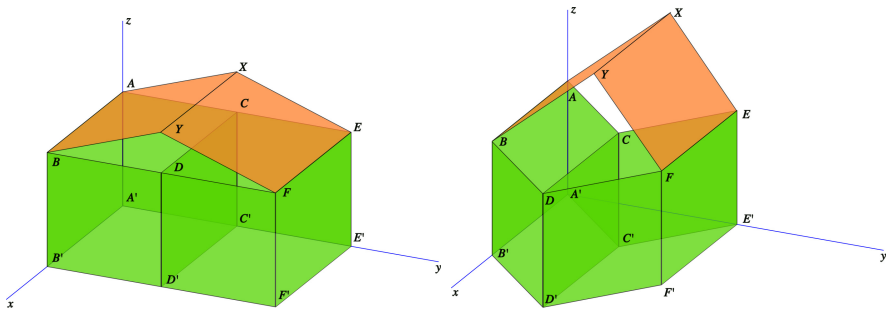

Figure 2.4: A polyhedral linkage which achieves a 1-dimensional range of motion.

The length of the edge XY is set to 1. All other new edges are given the same length, chosen to be some number larger than 1 so that the construction is embedded. The rectangles $ABYX$ and $EFYX$ constrain the vertices E and A to have the same x-coordinate. Therefore, the vertex E may move in the 1-dimensional region $\{0 \leq y \leq 2 \; ; \; x = 0 \; ; \; z = 1\}$. This is a notably simpler solution to linear motion in 3-dimensions than in 2-dimensions. Note that Sarrus' original linkage is obtained by removing the vertices D and D', and all edges and faces adjacent to them. (See [Sar53].) Our construction is more complicated, but having a third face parallel to the xz-plane allows for periodic extension.

We extend this construction periodically as follows. Note that in any realization of the previous linkage, the squares $EFF'E'$ and $ABB'A'$ are parallel translates of each other by a scalar multiple of the normal vector to each face. We attach multiple copies of the linkage together by identifying the $EFF'E'$ square on the i-th copy with the $ABB'A'$ square of the $(i+1)$-st copy.

With n copies attached, the E-vertex of the n-th copy can be moved within the region $\{0 \leq x \leq 2n; y = 0; z = 1\}$. Moreover, note that if we also add 'roofs' connecting the CD edge of the i-th copy to the CD edge of the $(i+1)$-st copy, then the y-coordinates of the C and D vertices of all constituent linkages will be the same, so they all will flex at the same rate. See Figure 2.5.

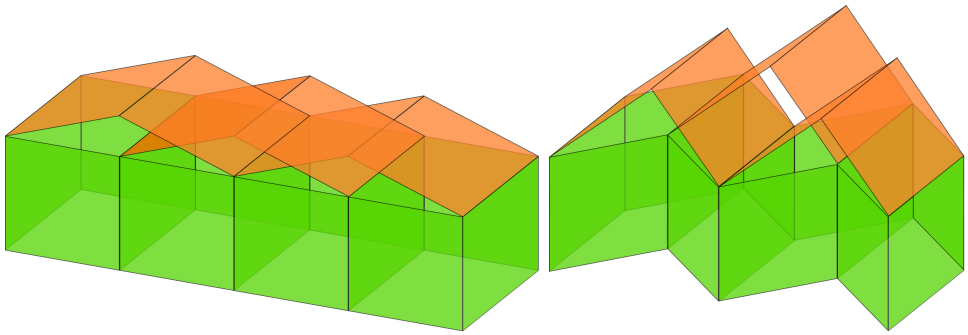

Figure 2.5: A portion of a periodic polyhedral linkage.

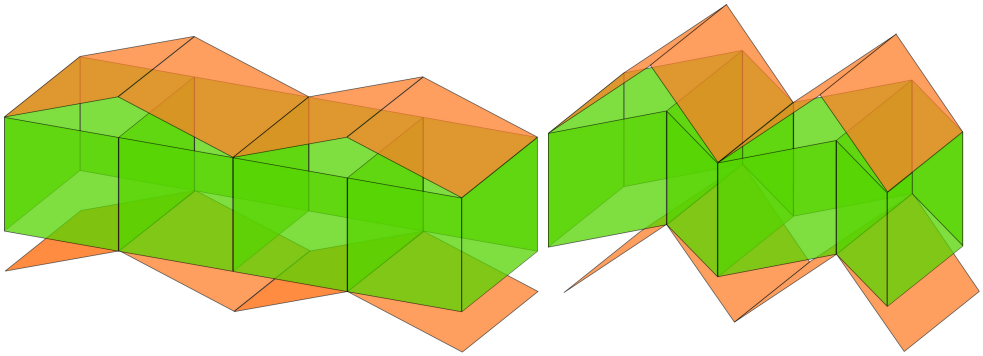

Figure 2.6: Portions of an embedded periodic polyhedral linkage.

Extending infinitely, we obtain a periodic polyhedral linkage whose configuration space is 1-dimensional, and whose periodicity is preserved during flexion. The direction of the periodicity vector does not change, only the magnitude. To embed this construction, we can attach some of the "roofs" to the bottom of the linkages. See Figure 2.6.

Restricting this linkage to a connected component of the embedded realization space $C^e(\mathcal{P}, f)$, we see that each periodic unit has a length in the range $(0, 2)$ as measured along the y-axis. Our construction gives the following theorem:

Theorem 2.3.1. *Let $0 < a < b$ and $\epsilon > 0$. There exists an embedded polyhedral linkage $\mathcal{P}$ with two faces F_1, F_2 and a 1-dimensional flex such that F_1 and F_2 remain parallel translates of each other during flexion while the distance between them varies continuously in the range*

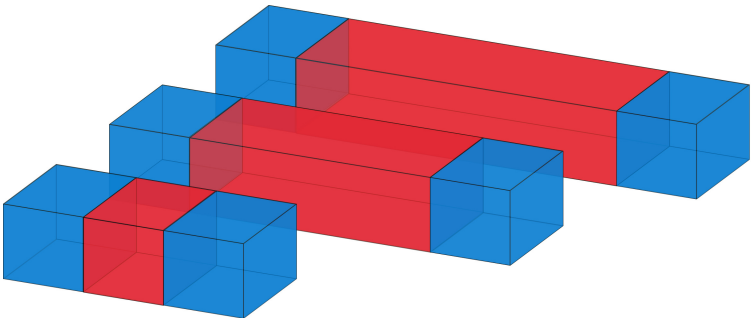

Figure 2.7: A set of extender linkages representing computational linkages.

(a, b), and $\mathcal{P}$ can be contained in a cylinder of radius ϵ and length b under any realization.

Proof. We scale our given construction so that the side length of each of the squares is a number d such that (1) under any flexion, each unit of the linkage is contained in a ball of radius ϵ, and (2) $b - a = N \cdot 2d$ for some integer N. Thus a linkage with N units, along with a rigid component of length a, will vary continuously in length between a and b. □

We call this construction an *extender linkage*. To simplify future figures, we represent an extender with a red rectangular prism which is understood to extend and contract in length. In contrast, blue faces are rigid faces and cannot be extended. (See Figure 2.7.)

2.4 Scalar computation

Suppose we have an array of extender linkages, pointed parallel to the y-axis in the xy-plane, and spaced at equal intervals so that the linkages never intersect under any realization. We fix one end of each extender on the x-axis and allow the other end to move freely parallel to the y-axis in a set range. Each linkage encodes a single real number represented by its length, and in this section we will describe how to use these extenders to perform computations on these inputs via embedded polyhedral linkages. (See Figure 2.7.)

Every extender linkage is taken to have the same range, (a, b), for two real numbers

$0 < a < b$ to be chosen later. The midpoint $m = \frac{1}{2}(a + b)$ is taken to represent 0, and in general, an extender linkage that is extended a distance y from the x-axis represents the value $y - m$. In this case we call the extender a *computational linkage* and say that $y - m$ is its *value*. We set $N = b - m$, so a computational linkage may represent any value in the range $(-N, N)$. The array of n computational linkages will be called a *register*. We refer to the individual computational linkages as $C_1, \ldots, C_n$ and their values as $[C_1], \ldots, [C_n]$, respectively.

Computations are decomposed into a sequence of elementary unary and binary operations which are performed on registers. Each operation takes one or two computational linkages as inputs, and stores its outputs in the values of another computational linkage. To embed this operation, computations are performed vertically. For a single operation, an output register is created, aligned in the xy-plane but offset vertically in the z-axis with respect to the input register. The output of the operation is attached to the output computational linkage in the output register. The values of all other original computational linkages are preserved by attaching each to their offset counterpart with rigid linkages.

Let $U \subset (-N, N)$ be a connected set and $f : U \to (-N, N)$ be a function. We say that we can *simulate* the function f by computational linkages if there is an embedded polyhedral linkage which connects an input computational linkage C_i to an output computational linkage C_i', such that if $[C_i] \in U$, then $[C_i'] = f([C_i])$. This definition also naturally generalizes if U is a connected subset of $(-N, N) \times (-N, N)$ using two input computational linkages C_i, C_j.

In the following subsections, we describe constructions which simulate elementary operations, including addition and multiplication by scalars, negation, addition, and multiplication. Together, these allow us to simulate any polynomial function on any bounded set.

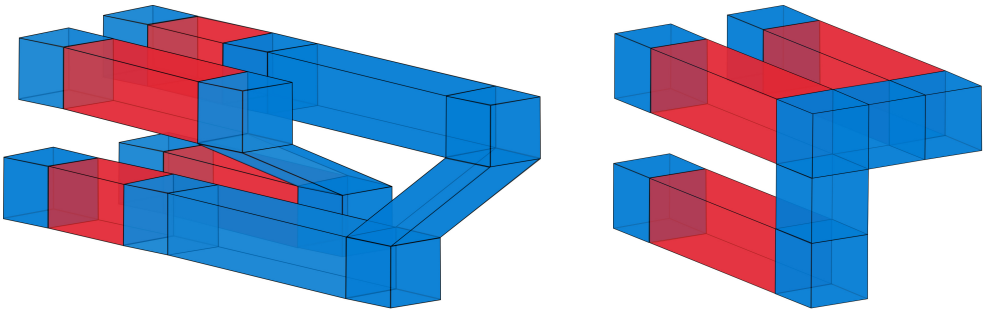

Figure 2.8: Left: a computational linkage which simulates a swap operation. Right: a computational linkage which simulates a copy operation.

2.4.1 Swap and copy

Before constructing polyhedral linkages to perform actual computations, we need to set up basic operations to manipulate memory stored in registers. We describe operations to swap two values stored in different computational linkages, as well as copy the value of one computational linkage to another.

Let $C_1, \ldots, C_n$ be the original computational linkages in the input register, and let $C'_1, \ldots, C'_n$ be the updated computational linkages in the output register. The swap operation s_i sends $[C_i] \mapsto [C'_{i+1}]$ and $[C_{i+1}] \mapsto [C'_i]$. For all $j \notin \{i, i+1\}$, we have $s_i : [C_j] \mapsto [C'_j]$. By composition, we can freely permute the computational linkages and so we will always assume that the input and output computational linkages are in a desirable configuration.

To simulate s_i, first C_i is connected to C'_{i+1} by a rigid set of parallelograms. However, the connection from C_{i+1} to C'_i needs to be rerouted to avoid intersecting with the C_i to C'_{i+1} connection. Thus we add a rectangular prism, which itself is rigid by the Cauchy Rigidity Theorem, of length at least $2N$ before adding the parallelograms to ensure that, under any realization, the operation is embedded. All other computational linkages are attached vertically by rectangles. (See Figure 2.8, left.)

A copy operation is comparatively simpler, because there is no need for rerouting. First,

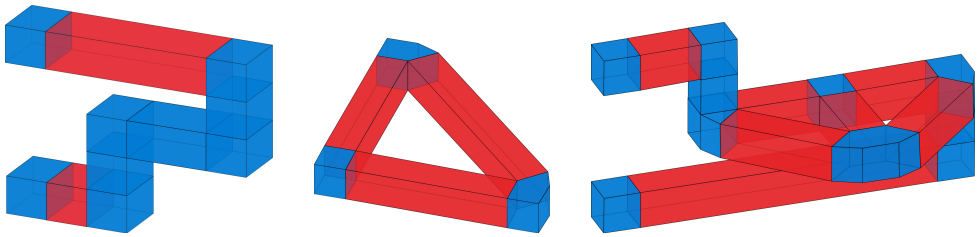

Figure 2.9: Left: a computational linkage for scalar addition. Middle: a $\left(\frac{\pi}{4}, \frac{\pi}{4}, \frac{\pi}{2}\right)$ triangle linkage. Right: a polyhedral linkage for negation.

C_i is connected to C_i' by a set of rectangles, and then C_i' is connected to C_{i+1}' by a rigid linkage. The entire construction is rigid, and all other computational linkages are attached vertically. (See Figure 2.8, right.)

Thus we can always assume without loss of generality that our linkages are in a desirable configuration. Usually, this means that input and output computational linkages are aligned vertically, or else are offset by one or two linkages. Additionally, we will assume enough space between linkages so that our constructions will always be embedded.

2.4.2 Scalar addition

For any constant λ, we can simulate the operation $x \mapsto x + \lambda$ on an appropriate domain by adding a rigid linkage.

Lemma 2.4.1. *For $\lambda \in (0, N)$, the function $x \mapsto x + \lambda$ on the domain $(-N, N - \lambda)$ and the function $x \mapsto x - \lambda$ on the domain $(\lambda - N, N)$ can be simulated by computational linkages.*

Proof. For $\lambda \in (0, N)$, we can define the operation of scalar addition via the linkage shown in Figure 2.9, left. A rigid structure is attached to the end of the computational linkage C_i, which adds an offset of length λ before attaching to the end of the new computational linkage C_i'. Subtraction is similar.

□

2.4.3 Negation

We can simulate the operation $x \mapsto -x$ on an appropriate domain by combining several extender linkages orthogonally.

Lemma 2.4.2. *The function $x \mapsto -x$ on the domain $(-\frac{1}{2}N, \frac{1}{2}N)$ can be simulated by computational linkages.*

Proof. We can simulate the operation of negation $x \mapsto -x$ on the domain $(0, N)$, by using two copies of the $\left(\frac{\pi}{4}, \frac{\pi}{4}, \frac{\pi}{2}\right)$ triangle linkage. (Figure 2.9, middle.) Extender linkages are attached at angle $\frac{\pi}{2}$ and connected by a third extender linkage, attached at angle $\frac{\pi}{4}$ relative to both legs. This constrains all three linkages to flex at the same rate, and the perpendicular sides will always be the same length. The negation linkage is formed by joining two $\left(\frac{\pi}{4}, \frac{\pi}{4}, \frac{\pi}{2}\right)$ triangle linkages along a common edge, enforcing the positive and negative legs to have the same length during all realizations. (See Figure 2.9, right.) The offset induced by the rigid central cube should be considered, but we can postcompose with a scalar addition operation. We leave the details to the reader.

Further, we can adjust the simulated domain to a neighborhood centered on 0 by precomposing and postcomposing with scalar addition $x \mapsto x + \mu$. The largest domain centered at 0 is obtained by choosing $\mu = N/2$, which lets us define a negation map on the domain $(-\frac{1}{2}N, \frac{1}{2}N)$. □

2.4.4 Scalar multiplication

For any constant λ, we can simulate the operation $x \mapsto \lambda x$ on an appropriate domain. The construction uses a pantograph, a fundamental linkage which scales the input using similar triangles. See Figure 2.10, left.

Lemma 2.4.3. *For $\lambda \in (1, N)$, the function $x \mapsto \lambda x$ on the domain $(-\frac{1}{2\lambda}N, \frac{1}{2\lambda}N)$ can be simulated by computational linkages. For $\lambda \in (0, 1)$, the functions $x \mapsto \lambda x$ on the domain*

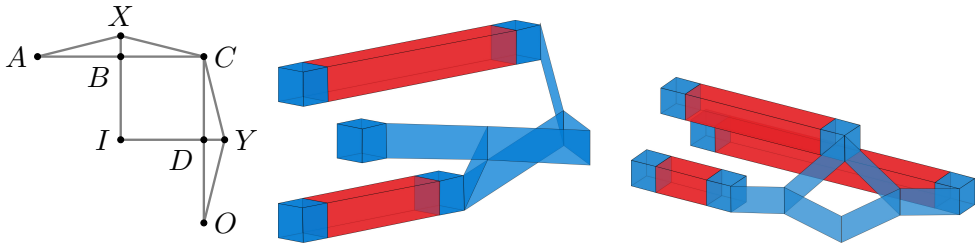

Figure 2.10: Left: a rigidifed pantograph, which is used for scalar multiplication and half-addition. Middle: a computational linkage for scalar multiplication. Right: a computational linkage for half-addition.

$(-\frac{1}{2}N, \frac{1}{2}N)$ can be simulated by computational linkages.

Proof. We prove the case when $\lambda \in (1, N)$ first. Consider the *pantograph* linkage in Figure 2.10, left. We fix the lengths $|AC| = \lambda|AB|$ and $|CO| = \lambda|DO|$. Vertex A is fixed at the origin, I is used as an input vertex, and O is used as an output vertex. The structure is *rigidified* so that the pairs of edges AB, BC and CD, DO remain parallel. To preserve embeddedness, this is achieved by adding the auxiliary vertices X and Y along with the triangles ABX, BCX, CDY and DOY. From the geometry of the construction, the linkage constrains $|AI| = \lambda|AO|$, achieving scalar multiplication. (See [KM02] §6.2)

We take this construction and extrude it to three dimensions. (See Figure 2.10, middle.) Vertices corresponding to A are fixed at the 0 value of the register. The input vertices corresponding to I are offset below and attached to a computational linkage in the previous register. The output vertices corresponding to O are offset above and attatched to a computational linkage in the next register. (Note: for figure clarity, we do not include the extrusion of the auxiliary vertices corresponding to X and Y, and the details of rigidifying are left to the reader.) Because $|AO| = \lambda|AI|$ in the original planar linkage, the same is true for the distances projected along the y-axis in the polyhedral linkage, thus it simulates the operation $x \mapsto \lambda x$ on the domain $(0, \frac{N}{\lambda})$. Here the domain is limited because nonpositive inputs would cause self intersections.

As with negation, we can adjust the simulated domain to include a neighborhood of 0 by precomposing with $x \mapsto x+\mu$ and then postcomposing with $x \mapsto x-\lambda\mu$. The largest domain centered at 0 is obtained by choosing $\mu = \frac{N}{2\lambda}$, which lets us define scalar multiplication on the domain $(-\frac{N}{2\lambda}, \frac{N}{2\lambda})$. Lastly, we can handle multiplication by $\lambda \in (0,1)$ by switching the input and output computational linkages. This is the same process as in planar linkages. (See [KM02] §6.2) Also note that in this case we can initially simulate the operation $x \mapsto \lambda x$ on the domain $(0, N)$ instead of $(0, \frac{N}{\lambda})$, which leads to the optimal value $\mu = \frac{N}{2}$. □

2.4.5 Addition

We can simulate the operation $(x, y) \mapsto x + y$ on an appropriate domain by using a modified pantograph to perform the operation $(x, y) \mapsto \frac{1}{2}(x+y)$, which we call *half-addition*, and then postcomposing with multiplication by 2.

Lemma 2.4.4. *The function $(x, y) \mapsto x + y$ on the domain $(-\frac{1}{4}N, \frac{1}{4}N) \times (-\frac{1}{4}N, \frac{1}{4}N)$ can be simulated by computational linkages.*

Proof. For planar linkages, we can reuse the pantograph to simulate the function $x,\ y \mapsto \frac{1}{2}(x+y)$. (Figure 2.10, left.) Here we fix $\lambda = 2$ and now take the vertices A and O to be inputs and the vertex I to be the output. (See [KM02] §6.3) As with scalar multiplication, we extrude the linkage to three dimensions and offset the input and outputs vertically. Here the input vertices corresponding to A and O are attatched to computational linkages in the previous register, and the output vertices corresponding to I are offset vertically and attached to a computational linkage in the new register. (See Figure 2.10, right.)

We can simulate the operation $(x, y) \mapsto x+y$ by postcomposition with $x \mapsto 2x$. Multiplication by 2 is defined on the domain $D := \{x, y \in (-N, N) \mid \frac{1}{2}(x+y) \in (-N/4, N/4)\}$. The largest square domain containing $(0, 0)$ in D is $(-N/4, N/4) \times (-N/4, N/4) \subset D$, which gives the simulation of the function $(x, y) \mapsto x+y$ on the domain $(-N/4, N/4) \times (-N/4, N/4)$. □

Remark: This proves the stronger statement that we can simulate $(x, y) \mapsto x + y$ on the domain D. We use this fact to simplify the construction of other linkages when we have knowledge about the inputs x and y. However, in general, we want a definition of the operation whose domain is not dependent on its inputs, and the choice is inconsequential because we will later choose N large enough to neglect this potential inefficiency.

2.4.6 Inversion

We can simulate the operation $x \mapsto \frac{1}{x}$ on an appropriate domain by using a modification of the elementary planar linkage known as a *Peaucellier inversor.*

Lemma 2.4.5. *The function $x \mapsto \frac{1}{x}$ on the domains $(1, N)$ and $(\frac{1}{N}, 1)$ can be simulated by computational linkages.*

Proof. Consider the planar linkage shown in Figure 2.11, left, which is called a *Peaucellier Inversor.* The vertex A is fixed at the origin. The vertex I is used as an input vertex and the vertex O is used as an output. From the geometry of the construction, we see that $|AO| = \frac{t^2}{|AI|}$ where $t^2 = |AC|^2 - |CO|^2$, and all the internal edges $|CO| = |CI| = |BO| = |BI|$. We choose edge lengths such that $t^2 = 1$. Note that the classical Peaucillier inversor is subject to degenerate configurations when the square $CIBO$ collapses. (See Kapovich and Millson's use of a 'hook' to prevent this in [KM02] §6.4) In our case, however, restricting to the embedded realizations prevents this collapse, so no special treatment is needed. (See also §2.6.3.) However, the embedded condition prevents opposite edges of the Peaucellier inversor from colliding, meaning we cannot simulate inversion at 1.

The input vertices corresponding to I and the output vertices corresponding to O are offset and attatched to computational linkages in different registers. See Figure 2.11, right. For clarity, the figure is drawn on its side. Choosing appropriate edge lengths, we can simulate the function $x \mapsto \frac{1}{x}$ on the domains $(1, N)$ (or $(\frac{1}{N}, 1)$ if we switch the input and outputs) where the bounds come from the intersection at $x = 1$ and the possible values

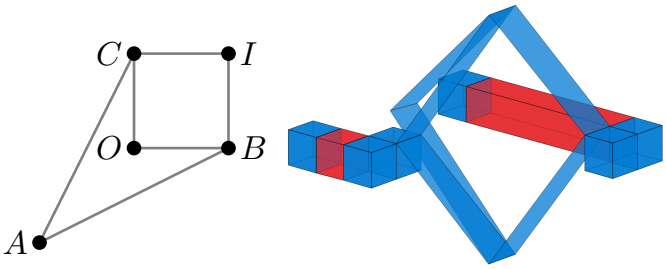

Figure 2.11: Left: a Peaucellier inversor, which is used for inversion. Right: a computational linkage for inversion.

representable on computational linkages. □

In this case, we do not worry about finding a symmetric domain centered at 0 because we will never use this linkage directly. We only simulate the operation $x \mapsto \frac{1}{x}$ in order to simulate the operations $x \mapsto x^2$ and $(x, y) \mapsto xy$ as follows.

2.4.7 Multiplication

We can simulate the operation $(x, y) \mapsto xy$ on an appropriate domain by using inversion and algebraic identities. To simplify notation, let

$$N^* = \frac{1}{2}\left(\sqrt{N} - 2\right)$$

with the assumption that $N > 4$ for the rest of this section. Importantly, N^* grows asymptotically as $\sqrt{N}$, so we can always choose a large enough value of N to perform all computations.

Lemma 2.4.6. *The function $x \mapsto x^2$ on the domain $(-N^*, N^*)$ can be simulated by computational linkages.*

Proof. We use the identity

$$\frac{1}{2}\left(\frac{1}{x-1} - \frac{1}{x+1}\right) = \frac{1}{x^2-1}$$

Thus we can simulate the function $x \mapsto x^2$ by composing with scalar addition, inversion, negation, and addition. The domain is only restricted by the scalar addition and inversion. For inversion, we choose to invert on the domain $(1, N)$, which gives us the requirement $2 < x < N - 1$. Note that we only use half-addition,

$$\left(\frac{1}{x-1},\ \frac{-1}{x+1}\right) \mapsto \frac{1}{2}\left(\frac{1}{x-1} + \frac{-1}{x+1}\right)$$

which is defined on the domain $(-N, N) \times (-N, N)$. No additional restrictions are imposed by negation because $\frac{1}{N} < \frac{1}{x+1} < \frac{1}{3}$ from the inversion requirements. To recover x^2 as the final output, we invert again and compose with scalar addition. For this to be well defined, we obtain the aditional constraint that $x < \sqrt{N}$.

In total, we can simulate the function $x \mapsto x^2$ on the domain $\left(2, \sqrt{N}\right)$. To adjust this domain to include 0, we can precompose with $x \mapsto x + \mu$ and postcompose with $y \mapsto y - 2x\mu - \mu^2$, where x is the original input to the function. The optimal μ is the average of the endpoints,

$$\mu = \frac{1}{2}\left(\sqrt{N} + 2\right)$$

giving the largest symmetric domain containing 0 as $(-N^*, N^*)$. With this value of μ, no additional restrictions come from the pre or postcomposition. □

Lemma 2.4.7. *The function $(x, y) \mapsto xy$ on the domain $(-\frac{1}{2}N^*, \frac{1}{2}N^*) \times (-\frac{1}{2}N^*, \frac{1}{2}N^*)$ can be simulated on computational linkages.*

Proof. We use the identity

$$\frac{1}{2}\left((x+y)^2 - (x-y)^2\right) = xy$$

Thus we can simulate the function $x, y \mapsto xy$ by composing addition, negation, and squaring. The composition of adding x and y and then squaring adds a new restriction on the domain, so we require that $x, y \in (-\frac{1}{2}N^*, \frac{1}{2}N^*)$. The other operations do not impose any new restrictions, where again we note that in the last step we use half-addition, $x, y \mapsto \frac{1}{2}(x+y)$, which is defined everywhere. □

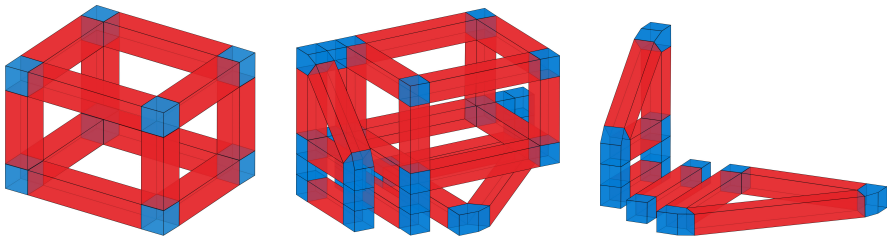

Figure 2.12: Left: an embedded polyhedral linkage with a 3-dimensional flexion. Middle/Right: a mechanism for translating 3 dimensional motion into computational linkages.

2.4.8 All polynomials can be simulated by computational linkages.

With the above constructions, we can simulate any polynomial function on an appropriate domain.

Theorem 2.4.8. *Let $f : \mathbb{R}^n \to \mathbb{R}^m$ be a polynomial function and $U \subset \mathbb{R}^n$ be a bounded set. Then we can simulate (f, U) by computational linkages.*

Proof. A polynomial function comes from the composition of scalar addition, scalar multiplication, negation, addition and multiplication. Each operation can be simulated by computational linkages, and for each operation, the domain is defined on some neighborhood of 0 whose size only depends on N. Thus we can choose N large enough that each operation is always defined on every input from U. □

2.5 Vector computation

For 3-dimensional motion, we consider the 1-skeleton of a cube made of twelve extender linkages joined by eight rigid cubes. (See Figure 2.12, left.) If one cube is fixed, the opposite cube has a 3-dimensional range of motion. Moreover, note that if this cube records the position (x, y, z), then the three cubes adjacent to the fixed cube record the coordinates $(x, 0, 0), (0, y, 0)$ and $(0, 0, z)$.

By adding two $\left(\frac{\pi}{4}, \frac{\pi}{4}, \frac{\pi}{2}\right)$ triangle linkage, we can transfer 3 dimensional motion to an array of three computational linkages. By offsetting the linkages, this construction can be embedded. (See Figure 2.12 middle, right.)

Conversely, we can also take three computational linkages C_1, C_2, C_3 and simulate three dimensional motion with a vertex aligned at $([C_1], [C_2], [C_3])$. This proves a generalization to the result given in one dimension on computational linkages.

Theorem 1.1. *Let $F : \mathbb{R}^{3m_1} \to \mathbb{R}^{3m_2}$ be a polynomial function, and $U \subset \mathbb{R}^{3m_1}$ be a bounded open set. There exists an embedded polyhedral linkage which realizes F on U.*

We can also restrict a polyhedral linkage to trace out a semialgebraic set.

Corollary 1.2. *Let $V \subset \mathbb{R}^3$ be an algebraic set, and $U \subset \mathbb{R}^3$ be a bounded subset. Then there is a fixed embedded polyhedral linkage which realizes $V \cap U$.*

Proof. An algebraic set V is defined as the vanishing locus of a set of polynomials $f_1, \ldots, f_n : \mathbb{R}^3 \to \mathbb{R}$. Let F be the function $\mathbb{R}^3 \to \mathbb{R}^{3n}$ defined by

$$F : (x, y, z) \mapsto \big((f_1(x, y, z), 0, 0), \ldots, (f_n(x, y, z), 0, 0)\big)$$

In this linkage we fix all of the output vertices to be at their relative origins $(0, 0, 0)$, thus for each f_i, we have the constraint that $f_i(x, y, z) = 0$. Thus the input vertex is constrained to be in the intersection $V \cap U$, completing the proof. □

2.6 Final remarks

2.6.1 Higher dimensions

Note that our proofs for Theorem 2.1.1 and Corollary 2.1.2 naturally generalize to all dimensions $n > 3$. By extruding a polyhedral linkage into higher dimensions, no added flexibility is gained. Thus by extruding our construction of extender linkages, we can generalize the

results of Theorem 2.3.1 into higher dimensions. Each step for performing scalar computation will carry over as well. And finally, we can modify our construction of translating 3-dimensional motion into computational linkages by employing the 1-skeleton of an n-cube made of extender linkages to translate n-dimensional motion into a register of n computational linkages, as in Figure 2.12. Thus our results hold for embedded polyhedral linkages in dimension $n \geq 3$.

2.6.2 Embedding planar linkages

The Peaucellier inversor is the main barrier to embedding planar linkages in Kempe's original proof. Although the Peaucellier inversor itself is planar, because the output vertex A is not adjacent to the external face, after any composition the resulting planar linkage will not correspond to a planar graph. (See Figure 2.11.) Thus any planar linkage which represents a polynomial of degree ≥ 2 cannot be embedded in $\mathbb{R}^2$ via Kempe's construction. An embedded construction was recently achieved in [AD+16].

However, note that deciding if a planar linkage can be embedded is different than deciding if the underlying graph is planar. Fáry's Theorem [Fáry48] states that every planar graph can be drawn in the plane using straight lines, so every planar graph can be realized by a linkage for some choice of edge weights. However, there exist planar linkages embedded in $\mathbb{R}^3$ which are topologically equivalent to the unknot but which cannot be moved to a convex realization. Such linkages are called *locked*. (See e.g. [CJ98] and [BD+98].) This phenomena is special to three dimensions; there are no locked planar linkages in two dimensions or four dimensions. (See [CDR03] and [CO01].)

With suitable hypotheses, Wilson [Wil12] proved a generalization of Fáry's Theorem for topological simplicial complexes in $\mathbb{R}^n$. Because polyhedral linkages have less flexibility than planar linkages, the existence of locked planar linkages in $\mathbb{R}^3$ implies that the same is true for 2-dimensional polyhedral linkages.

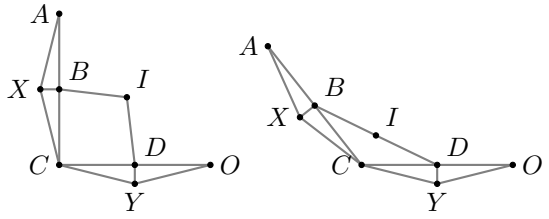

Figure 2.13: A skew pantograph that achieves a bounded flexible angle.

2.6.3 Embedded realizations

In § 2.2, we chose the convention to only consider the subset of embedded realizations so that the resulting linkages could be realized as physical mechanisms. An alternate approach is to constrain the linkages so that only embedded realizations are possible. (See e.g. [AD+16] for similar considerations for planar linkages in $\mathbb{R}^2$.)

Consider a rigidified pantograph, with $|BI| = |DI| < |BC| = |CD|$. (See Figure 2.13.) If $t = \frac{|BI|}{|BC|}$, then the angle $\angle ACO$ can open to a maximum measure of $2\sin^{-1}(t) < \pi$. Thus another way to prevent degenerate realizations of the square planar linkage is to replace each corner of the square with a copy of the skew pantograph. Then no degenerate realization is possible because every angle of the original square is strictly less than π. Extruding to a 3-dimensional polyhedral linkage gives a linkage whose entire configuration space is embedded. So one could provide an alternate proof of Theorem 2.3.1 based on this construction and produce an extender linkage whose entire realization space is embedded.

CHAPTER 3

Fully flexible 3-periodic polyhedral surface

3.1 Introduction

Flexibility is an unexpected property of some polyhedra. That is, a polyhedra is *flexible* if it has a continuous family of realizations containing the same combinatorial data: congruent faces, edges and vertices, all attached in the same manner, but which are pairwise not congruent under rigid motions. A polyhedra which is not flexible is called *rigid*.

One should expect *most* polyhedra to be rigid. To make this precise, one needs a way to parameterize polyhedra. Let $G = (V, E)$ be a plane triangulation, and let $\ell : E \to \mathbb{R}_{>0}$ be a length function on the edges. If ℓ satisfies the triangle inequality on each triangle of G, then the data (G, ℓ) defines a polyhedron. Let $\mathcal{L}(G)$ be the set of all such length functions ℓ, i.e., $\mathcal{L}(G)$ is the set of all realizations, up to rigid motions, of polyhedra with the combinatorial data given by G. Then for any planar triangulation G, the set of flexible realizations in $\mathcal{L}(G)$ has measure zero. See [Glu75], also [Poz60]. There are also broad clases of polyhedra which are known to be rigid. Most notably, a funamental result of Cauchy shows all convex polyhedra are rigid. (See, e.g., [Pak09, §26])

However, flexible polyhedra do exist. The first examples were introduced by Bricard, who constructed three families of self-intersecting octahedra (see e.g. [Li18, §2.3] and [Pak09, §30]). Later Connelly constructed non-self-intersecting examples [Con77]. The smallest (in the number of vertices) currently known non-self-intersecting, flexible polyhedron has eight vertices [GG+24].

Recent work asks if additional properties on polyhedra impose more constraints on flexibility. For example, Gaiffulin and Gaiffulin showed that a 2-periodic infinite polyhedral surface homeomorphic to the plane has at most 1-dimension of flexibility [GG14]. Here we say that a flexible polyhedron has n-dimensions of flexibility if the continuous family of realizations has a neighborhood isomorphic to n-dimensional space.

The topological hypothesis is necessary here. Glazyrin and Pak provided a construction of a 2-periodic infinite polyhedral surface, not homeomorphic to the plane, which has 3-dimensions of flexibility [GP22]. Note that this is best possible while maintaining 2-perioidicity: the lengths of the two periodicity vectors may change, as well as the relative angle between them. In this paper, we extend this result by constructing a 3-periodic infinite polyhedral surface which has 6-dimensions of flexibility. Again, this is the best possible while maintaining 3-periodicity: the lengths of the three periodicity vectors may change, as well as the relative angles between any pair of them.

Another distinction is whether such a flexible polyhedral surface has any flexes which do not preserve periodicity. In the case that all flexes preserve periodicity and the dimension of flexibility is as large as possible, we say the surface is *strictly fully flexible*. When there are other flexes which do not preserve periodicity, we say that the surface is *non-strictly fully flexible*. In this paper, we present examples of both non-strictly fully flexible and strictly fully flexible 3-periodic polyhedral surfaces.

First, full definitions are given in Section 3.2. Importantly, we specify the metric used to define flexibility on infinite polyhedral surfaces, which is based on dihedral angles instead of the absolute position of vertices. (In a compact polyhedral surface, this distinction does not matter. However, for an infinite polyhedral surface, an arbitrarily small change of a dihedral angle may move a distant vertex an arbitrarily large amount.) Next the construction for a non-strictly fully flexible 3-periodic polyhedral surface is given in Section 3.3. This is an extension of the 2-periodic construction given by Glazyrin and Pak in [GP22]. The strictly fully flexible 3-periodic construction is based on the notion of polyhedral linkages, which are

described in Section 3.4. Here we give a construction of a polyhedral linkage which satisfies the strictly fully flexible conditions. Then in Section 3.5 we describe a transformation which produces a polyhedral surface from a polyhedral linkage while preserving the conditions of being strictly fully flexible and 3-periodic.

3.2 Definitions and notations

Let K be a polyhedral connected pure 2-dimensional complex, where each 2-dimensional cell is a convex polygon. By a *polyhedral surface* we mean a pair (K, θ), where $\theta : K \to \mathbb{R}^3$ is a mapping linear on each polygon of K. In other words, a surface is a realization of the complex K in $\mathbb{R}^3$. For a given complex K, we define the space of its realizations $\mathcal{S}(K)$. In this paper we study flexible polyhedral surfaces. In case K is a finite complex homeomorphic to a sphere, (K, θ) is a compact polyhedron in $\mathbb{R}^3$. A closed polyhedron $S = S_0$ is called *flexible*, if there is a continuous family $\{S_t, t \in [0, 1]\}$, of polyhedra realizing the same polyhedral complex that are not pairwise congruent in $\mathbb{R}^3$.

We are, however, mostly interested in flexible infinite polyhedral surfaces. The definition of a flexible polyhedron provided above is not directly transferable to the unbounded case so we have to be a bit more careful defining flexible infinite surfaces. For a fixed polyhedral complex K, we define a metric on $\mathcal{S}(K)/\text{Isom } \mathbb{R}^3$ based on dihedral angles of a surface. Let $(e_1, e_2, \ldots)$ be an arbitrary ordering of edges in K. For each surface in $S \in \mathcal{S}(K)/\text{Isom } \mathbb{R}^3$, we record the sequence of its dihedral angles $\alpha(S) = (\alpha_1, \alpha_2, \ldots)$ according to this particular ordering. Then for two surfaces $S_1, S_2 \in \mathcal{S}(K)/\text{Isom } \mathbb{R}^3$ the distance between them is $||\alpha(S_1) - \alpha(S_2)||_\infty$. A polyhedral surface $S = S_0 \in \mathcal{S}(K)/\text{Isom } \mathbb{R}^3$ is *flexible*, if there is a continuous (with respect to the topology from the metric defined above) family of pairwise distinct $\{S_t, t \in [0, 1]\}$ in $\mathcal{S}(K)/\text{Isom } \mathbb{R}^3$. This family $\{S_t\}$ is called a *flex* of S. More generally, we say that a n-dimensional flex is a family $\{S_t, t \in [0, 1]^n\}$, and the *dimension of flexibility* if the largest n such that S has an n-dimensional flex. A surface S_t for a concrete

value of S is called a *flexor* of S. A non-flexible surface is also called *rigid*.

We are particularly interested in polyhedral surfaces preserved by lattice translations. Let K be a polyhedral connected pure 2-dimensional complex with a free action of the group $G = \mathbb{Z} \oplus \mathbb{Z} \oplus \mathbb{Z}$ with generators a, b, and c. Assume that G acts as a linear bijective map on each cell of K, and that the number of orbits of the action of G is finite. Let $\theta : K \to \mathbb{R}^3$ be a linear map on each cell of K equivariant with respect to the action of $\mathbb{Z} \oplus \mathbb{Z} \oplus \mathbb{Z}$, such that a, b, and c act by translations with vectors α, β, and γ respectively. Then the pair (K, θ) is called a *3-periodic polyhedral surface*.

For the periodicity vectors α, β, γ of a 3-periodic polyhedral surface $S = (K, \theta)$, let Λ be the lattice generated by α, β, and γ, that is $\Lambda = \{x\alpha + y\beta + z\gamma : (x, y, z) \in \mathbb{Z}^3\}$. We say that a flex of (K, θ) is 3-periodic if all flexors S_t, $t \in [0, 1]$ are also 3-periodic. The lattice Λ is defined (up to isometries of $\mathbb{R}^3$) by the Gram matrix of its generating vectors, that is, by 6 pairwise inner products between α, β, and γ. A natural topology on the space of lattices is inherited from the topology of $\mathbb{R}^6$ based on these 6 inner products. We say that a 3-periodic polyhedral surface S is *fully flexible* if there is a neighborhood of Λ in the space of lattices such that for any lattice Λ' from this neighborhood, there is a 3-periodic flex S_t of S where the corresponding lattice of the flexor S_1 is Λ'. We say that a 3-periodic polyhedral surface is *strictly fully flexible* if it is fully flexible, all its flexes are 3-periodic, and, given Λ' from the neighborhood of Λ, there is a unique flexor with the underlying lattice Λ' for all possible flexes S_t. Else, a surface is called *non-strictly fully flexible*.

With a slight change of definitions from above, one can also define 2-periodic surfaces and their full flexibility. One of the results in [GP22] is the construction of a fully flexible 2-periodic triangular surface which answered the question of Gaifullin and Gaifullin [GG14] in the negative. Note that the construction from [GP22] is non-strictly fully flexible.

3.3 Non-strictly fully flexible 3-periodic surfaces

In this section we construct a non-strictly fully flexible 3-periodic surface. The main ideas behind this construction are similar to those used for a fully flexible 2-periodic surface in [GP22]. Although not strictly necessary for this particular construction, it always makes sense to keep in mind the fundamental result of Cauchy: the surface of any convex polyhedron is not flexible (see, for instance, [Pak09, §26]). Our construction will be glued from many polyhedral pieces and those of them that are directly obtained from convex polyhedra do not add anything to the space of flexes.

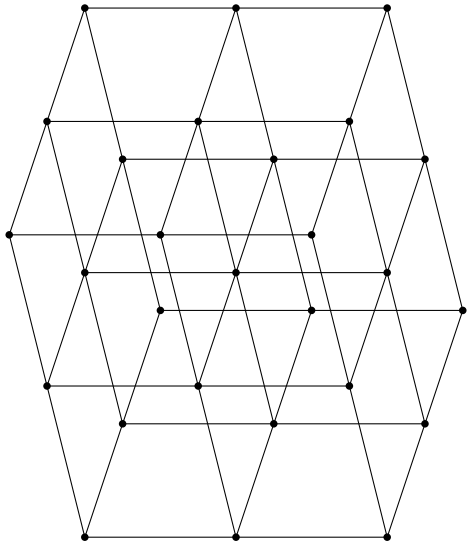

Figure 3.1: A $3 \times 3 \times 3$ piece of the lattice complex.

For the first step of the construction, we start with an arbitrary lattice Λ with basis vectors α, β, and γ and connect by a line segment any pair of vertices in Λ whose difference is either α, β, or γ. This creates a 1-dimensional complex where every vertex has exactly 6 edges (see a piece of the complex in Figure 3.1).

For the second step, we thicken the 1-dimensional lattice complex by substituting each interval by a triangular prism and each vertex by a convex polyhedron that is the convex hull

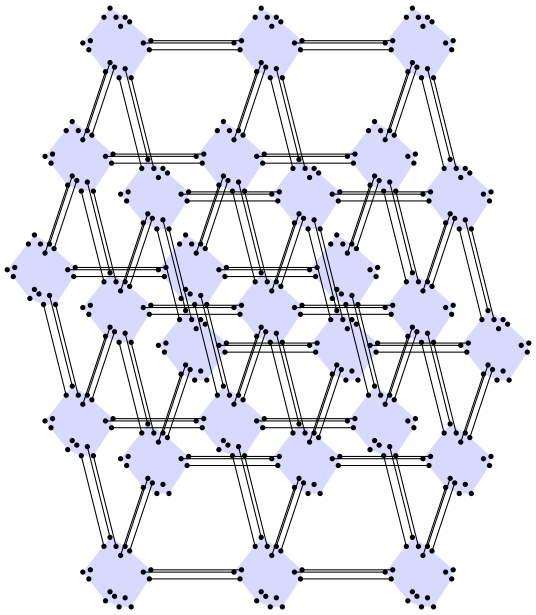

Figure 3.2: Thickened complex with connector nodes and triangular prisms as struts.

of six triangles (see Figure 3.2). It is not difficult to see that one can make the construction where all prisms are right and have equilateral triangles as bases so, for simplicity, we will use only these in our proof. At this stage the structure reminds of various geometric construction set toys, where connector nodes (blue polyhedra in Figure 3.2) are connected by struts/tubes (triangular prisms).

The next step is arguably the most important in the construction. We substitute each triangular prism by a flexible polyhedron with two parallel triangles as its facets such that the space of its flexes contains the whole 3-dimensional neighborhood of relative positions of these two triangles with respect to each other. The existence of such a polyhedron is formalized by the following lemma.

Lemma 3.3.1. *For any $\varepsilon > 0$, there exists a flexible polyhedron P satisfying the following conditions: 1) P has two triangular facets Δ_1 and Δ_2 that are both equilateral triangles with sides ε and $\Delta_2 = \Delta_1 + u$, where u is a unit vector orthogonal to the plane of Δ_1; 2) for any vector u' from the neighborhood of u, there exists a flex of P that has Δ_1 fixed and moves*

Δ_2 *to* $\Delta_1 + u'$.

Proof. By scaling and gluing convex polyhedra to triangles, we can assume that ε is an arbitrary positive number and u is an arbitrary vector not contained in the plane of Δ_1. We take an arbitrary flexible polyhedron F with two adjacent faces f_1 and f_2 such that the angle between them changes during a flex. Then we glue a non-flexible polyhedron to f_2 with a centrally symmetric face s to get F' such that during a flex s is just rotated around f_1 (this can be done if the planes of f_1, f_2, and s share the same line). Now, we take a centrally symmetric image of F' and glue it to F' by s to obtain F''.

Consider flexes of F'' that keep its central symmetry, that is, both F' and its symmetric image are simultaneously flexed using the same flex. Then, if we assume the facet f_1 is fixed, its centrally symmetric counterpart f_1'' is moving along a circular trajectory. Assume v is the tangent vector of this trajectory at the beginning of the flex. By making slight modifications to the construction, we can ensure that v is neither parallel to the plane of f_1 (this happens when s is initially orthogonal to f_1) nor perpendicular to the plane of f_1 (this happens when s is initially perpendicular to f_1).

We glue a polyhedron to f_1 and a polyhedron to f_1'' so that the new polyhedron has two equilateral triangular faces Δ and Δ', parallel translates of each other and both parallel to f_1. In a resulting polyhedron P', there is a flex that moves Δ' along a circle with the tangent vector v to the trajectory. At this point, we take three copies of P' obtained by the rotation by 0, $\pi/3$, and $2\pi/3$, respectively, preserving Δ. Gluing this three copies by associating corresponding Δ and Δ' in them, we finally get our polyhedron P. The flexing tangent vectors for these three copies are v, v' (v rotated by $\pi/3$), and v'' (v rotated by $2\pi/3$). Note that these three vectors form a basis of $\mathbb{R}^3$ because v is neither parallel nor orthogonal to the axis of rotation. This means that there is a combination of flexes from these three copies that produces a flex for any vector in the neighborhood of the translation vector between Δ (of the first copy of P') and Δ' (of the third copy of P'). □

Using Lemma 3.3.1 we can prove that our construction is a fully flexible 3-periodic surface.

Theorem 3.3.1. *For any lattice Λ, there is a fully flexible 3-periodic surface with underlying lattice Λ.*

Proof. We use the construction described above. Fix an arbitrary lattice Λ' in a sufficiently small neighborhood of Λ. For the flex of the whole surface depending on $t \in [0, 1]$, first define the transformation of convex connector nodes (blue polyhedra in Figure 3.2) as parallel translations linear with t such that the position for $t = 0$ corresponds to Λ and the position for $t = 1$ corresponds to Λ'. The remaining part is to show that there is a flex of all connecting tubes satisfying this movement of nodes. This follows immediately from Lemma 3.3.1. □

Remark 3.3.2. *It is easy to see that the construction in Theorem 3.3.1 can be made a triangular surface by carefully ensuring that all faces are triangles. It can also be made an embedded surface by taking sufficiently small connecting tubes and substituting them by embeddable flexible polyhedra lying strictly inside their corresponding tubes.*

In the construction of Theorem 3.3.1, the surface S/Λ has genus 3. The construction can be straightforwardly extended to the one, where S/Λ has any genus $g \geq 3$. Of course it is easy to construct a flexible surface of any genus by just attaching rigid polyhedral handles. It is more interesting to find a surface where the surface flexes along any loop. To formulate this more precisely, we say that an element of the fundamental group of the surface is *flexing in the surface* if for any corresponding loop of the surface composed of straight line segments, there is a flex of the surface such that some angles of the loop are changing during the flex.

Theorem 3.3.3. *For any lattice Λ and any $g \geq 3$, there is a fully flexible 3-periodic surface S with underlying lattice Λ of genus g such that g generating elements of the fundamental group of S/Λ are flexing in S.*

Proof. It is sufficient to follow the same process after adding more edges (primitive vectors of the lattice) to the 3-periodic 1-complex at the very beginning so that the degree of each

vertex is, initially, $2g$. The rest of the construction works just the same. □

Note that the constructions above are based on the existence of flexible polyhedra in $\mathbb{R}^3$. In particular, embeddable surfaces can be constructed using embeddable flexible polyhedra. The existence of embeddable flexible polyhedra is not known in all dimensions ≥ 4. However, we can construct fully flexible non-embeddable surfaces extending the construction of Theorem 3.3.1 by using flexible cross-polytopes, extensions of Bricard octahedra to higher dimensions (see [Gai14] for details).

All definitions are naturally extended from 3-dimensional definitions in Section 3.2 to the d-dimensional case.

Theorem 3.3.4. *For any lattice $\Lambda \subset \mathbb{R}^d$, there is a fully flexible d-periodic surface with underlying lattice Λ.*

Proof. The proof essentially follows the proof of Theorem 3.3.1. We construct a 1-dimensional d-periodic complex using basis vectors and then thicken it by substituting edges with simplicial prisms, where prisms have regular $(d-1)$-simplices as their bases. The main step is the analog of Lemma 3.3.1 in higher dimensions. The only difference in the proof of the lemma is in the very last step, where we need to glue d copies of the polyhedron P', instead of 3. It is clear that using permutations on the vertices of the regular $(d-1)$-simplex we can guarantee that the corresponding d vectors form a basis of $\mathbb{R}^d$ and, therefore, obtain the whole d-dimensional neighborhood of flexors using flexings of all d copies of P'. □

3.4 Polyhedral linkages

Before constructing a strictly fully flexible embedded 3-periodic polyhedral surface, we consider the simpler case of polyhedral linkages, which we define shortly. In this section, we give a construction for a strictly fully flexible, embedded, 3-periodic polyhedral linkage. In the next section, we describe how to modify this construction into a polyhedral surface while

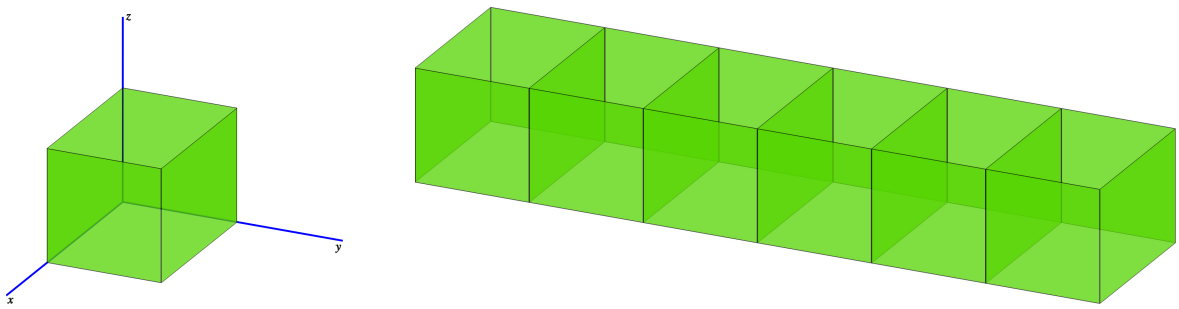

Figure 3.3: Example polyhedral linkages.

preserving the properties of being strictly fully flexible, embedded, and 3-periodic.

A *polyhedral linkage* is a collection of polygons attached in $\mathbb{R}^3$ along shared edges. This generalizes polyhedral surfaces (with boundary) by allowing three or more polygons to meet as a single edge. (Such an edge has no Euclidean neighborhood.) Note that polyhedral linkages are also a generalization of planar linkages from 2-dimensions to 3-dimensions, see Chapter 2. The definitions of being (strictly) fully flexible, embedded, and periodic are the same for polyhedral linkages as for polyhedral surfaces.

Now we begin constructing a gadget, which we call an *augmented chain*, which we use to construct a strictly fully flexible, embedded, 3-periodic polyhedral linkage. Consider the polyhedral linkage formed by removing two opposite faces of a cube. See Figure 3.3, left. This linkage has one dimension of flexibility. If we fix one square in the xz-plane, the opposite square may move but is constrained to remain parallel to the xz-plane. We call this linkage a *loop*.

Consider several loops, with the same orientation, attached together along shared faces. See Figure 3.3, right. Each loop link has an independent flex, but we can constrain the linkage to have just one dimension of flexibility in total. Take the ith and $i+2$nd squares parallel to the xz-plane. Attach one rectangle to each square along the top edge, and attach the two rectangles together. This forms a *roof* over the two loops. See Figure 3.4, with the roof shown in orange. As the linkage flexes, the roof enforces that the two squares share

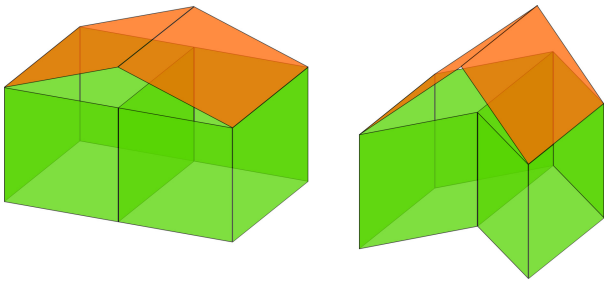

Figure 3.4: Adding a *roof* over two links.

the same x-coordinate. Thus the flex in the first loop is induced as an equal and opposite flex in the second loop, and overall the linkage has only 1 dimension of flexibility. Note that the linkage with infinitely many loops has a 1-periodic flex; the length of the periodicity vector varies, but the direction remains constant. We call this polyhedral linkage a *chain*. We summarize this in the following lemma.

Lemma 3.4.1. *A chain has one dimension of flexibility, and this flex is* 1*-periodic. If one square is fixed, then flexing the chain changes the length, but not the direction, of the periodicity vector.*

Note that we can embbed this structure by using skew parallelograms instead of rectangles for the roofs. See Figure 3.5. (We could also embedd this construction by placing half of the roofs on the opposite side of the chain, but we will need this space in the next construction.) For an embedded polyhedral linkage, we only consider flexes which preserve the embedding. In particular, we do not consider flexing a single link until it collapses into the xz-plane. However, to simplify future figures we illustrate chains with rectangles instead of parallelograms.

Next, we *augment* the chains as follows. Take two separate chains and orient them with periodicity vectors parallel to the y-axis, and with roofs facing in opposite directions along the z-axis. Stagger them apart by a unit distance in the z-axis, and add a square connecting each set of squares parallel to the xz-plane in the top and bottom chains. We call this

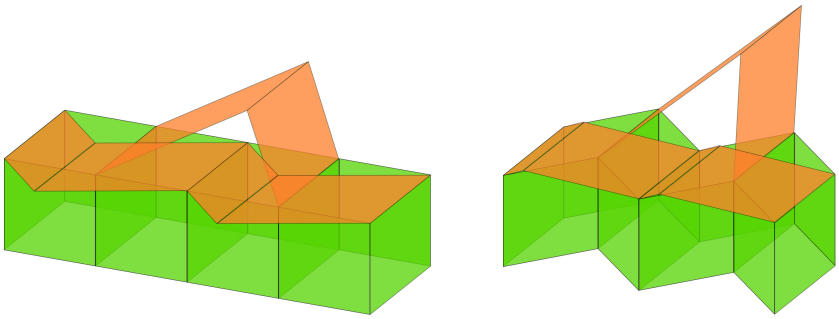

Figure 3.5: Using parallelograms to embed multiple roofs.

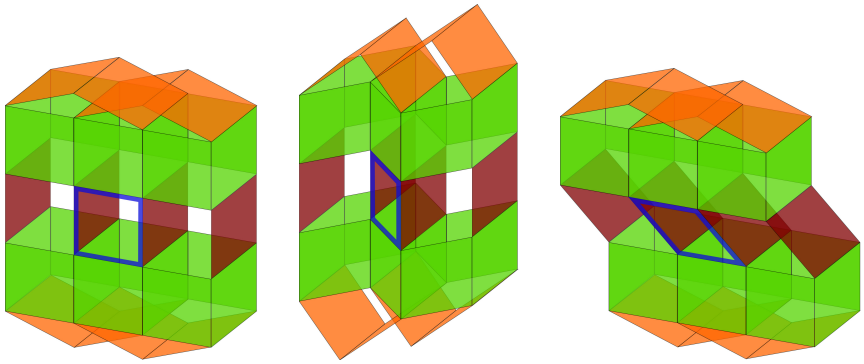

Figure 3.6: An augmented chain (left) with two independent flexes shown (center, right).

polyhedral linkage an *augmented chain*. The added squares are called *attaching squares*. See Figure 3.6, with the attaching squares shown in red.

Lemma 3.4.2. *An augmented chain has* 2 *dimensions of flexibility. Both flexes are* 1*-periodic. One flex changes the length, but not direction, of the periodicity vector. The other flex changes the angle of the attatching squares relative to the periodicity vector, which remains constant during this flex.*

Proof. Both chains can flex simulatenously, wich changes the length of the periodicity vector while the direction remains constant. (Shee Figure 3.6, middle.) And the two chains can move relative to each other by flexing the attaching squares relative to the periodicity axis, which does not change the periodicity vector. See Figure 3.6, right.

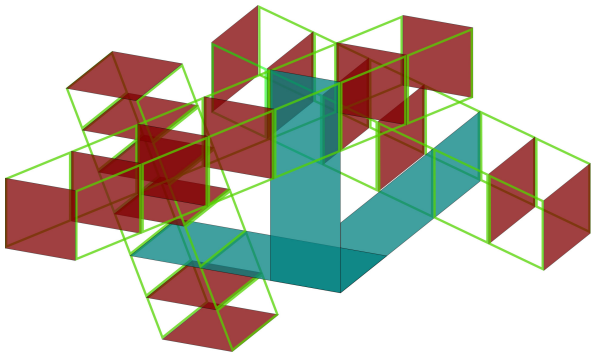

Figure 3.7: A *pivot* with three augmented chains attatched.

These are the only flexes of the augmented chain. To see this, note that all attaching squares remain parallel under any flex. The boundary component composed of any two consecutive attaching squares and the adjacent top and bottom loops forms a rhombus, shaded blue in Figure 3.6. In any flex, opposite edges of these rhombi are parallel, so the two attaching squares form the same angle with respect to the periodicity axis. Second, note that any flex in the upper chain is induced in the lower chain. Each attaching square enforces that its two adjacent squares in the top and bottom chains have the same x-coordinate, meaning that any flex in the upper linkage is transmitted to an equal flex in the bottom linkage, and vice versa. See Figure 3.6, middle.

□

Now we give a construction for a strictly fully flexible, embedded, 3-periodic polyhedral linkage. Our construction is for a lattice generated by an orthonormal basis, but we describe how this can be easily modified to fit an arbitrary basis.

Theorem 3.4.1. *For any lattice Λ, there is an embedded strictly fully flexible 3-periodic polyhedral linkage with underlying lattice Λ.*

Proof. First, we assume that Λ is generated by the standard basis vectors is $\mathbb{R}^3$. Attach three rectangles together around a central solid angle. This is aligned so that each rectangle

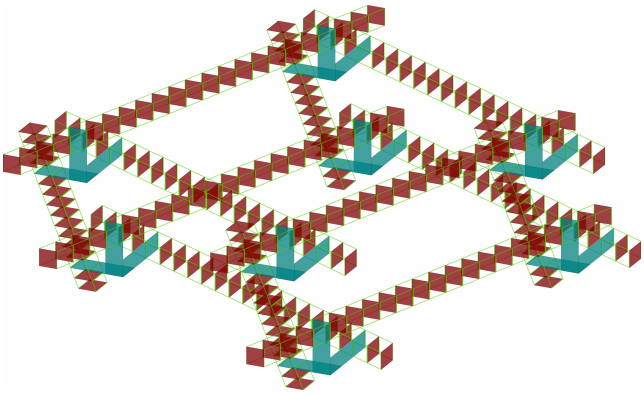

Figure 3.8: A portion of a fully flexible, embedded, three-periodic polyhedral linkage.

points along one of the three coordinate axes. We call this a *pivot*. Next, to each rectangle of the pivot, attach an augmented chain by using the rectangle in place of one of the attaching squares. This allows the three augmented chains to rotate in the plane perpendicular to each rectangle. E.g., for the rectangle oriented parallel to the x-axis, the augmented chain can rotate in the yz-plane. Note that all pivots remain aligned with the coordinate axes during flexes of the augmented chains. See Figure 3.7. For clarity, we simplify the drawing of each augmented chain by only including the attaching squares and boundary components of the adjacent loops. To make room for the loops and roofs in each augmented chain, one should take longer rectangles when constructing the pivot. We leave full details here to the reader.

We repeat this construction periodically along each augmented chain. At regular intervals, one attaching square is replaced by a rectangle, and three rectangles are attached along a central solid angle, creating a new pivot. This forms a three dimensional lattice. See Figure 3.8. This construction is easily modified for any lattice Λ by attatching the augmented chains to the pivots at different angles and using augmented chains of different relative lengths.

This linkage has 6 dimensions of flexibility. Each of the three sets of parallel augmented chains may change in length and in relative angle to the pivots by flexing the attaching squares. To see that no other flexes are possible, we show that a flex in any one augmented

chain will be induced in all parallel augmented chains. Without loss of generality, consider two adjacent augmented chains oriented parallel to the x-axis, crossed by a pair of augmented chains parallel to the y-axis. The two x-axis augmented chains must have the same flex in their attaching squares; if not, then at some distant point the attatched augmented chains parallel to the y-axis would flex beyond their maximal length. Thus all x-axis augmented chains remain parallel during flex. Moreover, the two x-axis augmented chains must have the same flex in their length; portions of the x-axis augmented chains and the crossing y-axis augmented chains form a parallelogram because the opposite angles are equal. Thus the opposite sides have the same length, so all x-axis augmented chains have the same length during flex. This is true of each set of axis oriented augmented chains, proving strict fully flexibility.

□

3.5 Strictly fully flexible 3-periodic surfaces

Now we describe a procedure to transform a polyhedral linkage into a polyhedral surface. The outline is to replace each polygon in the polyhedral complex with a polygonal prism. Each edge of the linkage where two or more polygons are attatched is replaced by a flexible polyhedral which acts as a hinge, allowing the surface to flex with the same behavior as the original linkage.

Begin with a flexible polyhedra with exactly one dimension of flexibility. For instance, take Tachi's flexible polyhedron, consisting of two tetrahedra attached with a crinkle fold. (See [Li18]) During flex, the relative angle of the two tetrahedra changes, see Figure 3.9. The range of motion of the two tetrahedra under optimal parameters is 80°, which is more than sufficient for our case.

We use this as a basis for constructing a polyhedral hinge. Attach a rectangular pyramid to each tetrahedra, such that the two rectangular faces rotate about a central axis as Tachi's

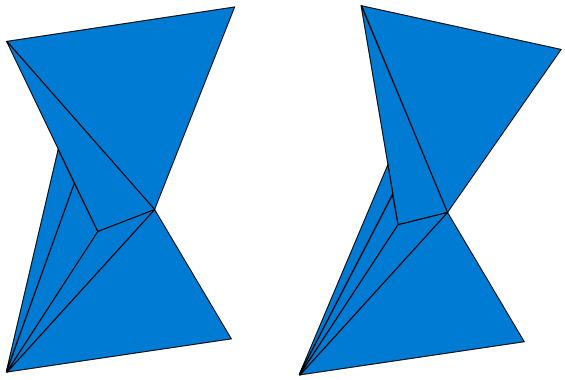

Figure 3.9: A flexible polyhedra.

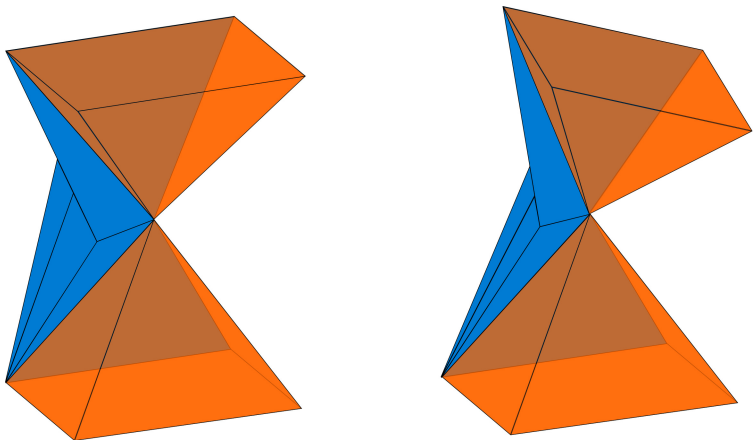

Figure 3.10: Creating a hinge using a flexible polyhedra.

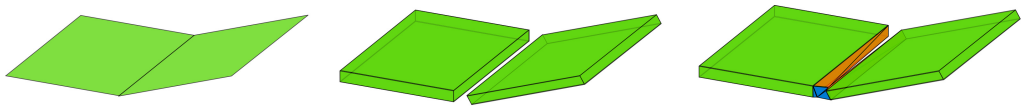

Figure 3.11: Replacing a polyhedral linkage with a flexible polyhedral surface.

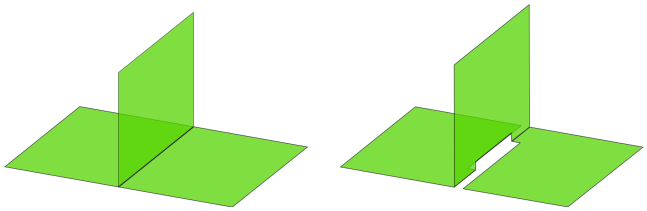

Figure 3.12: Refining an edge with three adjacent polygons to two edges with two adjacent polygons each.

polyhedron flexes. See Figure 3.10.

This allows us to replace polygons in our polyhedral linkage by polygonal prisms, and shared edges by a polyhedral hinge. See Figure 3.11. The only case to consider is when three or more polygons meet at a shared edge, but in this case we may *refine* the edge into several smaller edges so that only two polygons meet at a time. See Figure 3.12.

Because the flexible polyhedra used has only one flex, this exactly preserves the flexes of the original polyhedral linkage. Also note that because we have chosen an embedded flexible polyhedra, embedding is preserved as well. And periodicity follows immediately. So applying this procedure to our strictly fully flexible, embedded, 3-periodic polyhedral linkage constructed in the previous section yields the following result.

Theorem 3.5.1. *For any lattice* Λ*, there is an embedded, strictly fully flexible* 3*-periodic polyhedral surface with underlying lattice* Λ*.*

As a remark, note that we can strengthen this result to include a triangulated surface with a more detailed construction. The outline is to replace the rectangular prisms with a convex polygon, all of whose faces are triangles, of similar shape. Because this is convex,

there are no flexes of these polyhedra. To attatch two of these triangulated polyhedra, we assume they each have a congruent triangle, where we modify the construction of each if necessary. Then we remove these triangles from each polyhedron and glue them together along the boundary. Even without these faces, both polyhedra are still rigid because the triangle formed by the boundary of the removed faces are rigid.

3.6 Final remarks

One potential application of a strictly fully flexible periodic surface is in robotics. Here one cannot build a replica of an infinite polyhedral surface, but a finite portion which is periodic wherever periodicity is well defined. In this case, being fully flexible means that the three periodicity vectors can be changed independently, and being strictly fully flexible means that any local change in one part of the structure is induced as a global change in the entire structure. E.g., one could drive the behavior of the entire structure by attaching motors to one part of the structure. There would be no need to synchronize multiple motors in multiple locations to enforce periodicity.

However, our construction needs to be infinite in order to be strictly fully flexible. In the proof of Theorem 3.4.1, we enforce that a flex in one augmented chain is induced in all parrallel augmented chains by appealing to a crossing augmented chain at an arbitrarily far distance. For a finite portion of the surface, this argument does not work. Instead, there is some possible error whose magnitude is inversly related to the size of the entire linkage. An area for future work would be to construct a strictly fully flexible 3-periodic polyhedral surface with the additional property that any finite portion is also strictly fully flexible and 3-periodic, wherever periodicity is well defined.

REFERENCES

[Abb08] T. Abbott, Generalizations of Kempe's universality theorem, Masters thesis, Massachusetts Institute of Technology, Dept. of Electrical Engineering and Computer Science, 2008, 86pp. URL: https://web.mit.edu/tabbott/www/papers/mthesis.pdf.

[AD+16] Z. Abel, E. Demaine, M. Demaine, S. Eisenstat, J. Lynch, and T. B. Schardl Who Needs Crossings? Hardness of Plane Graph Rigidity. In: *Proceedings of the 32nd International Symposium on Computational Geometry (SoCG)*, Boston, MA June 2016, 3:1-15.

[AK24] S. Anan'in, D. Korshunov, Moduli spaces of polygons and deformations of polyhedra with boundary, *Geom. Dedicate* **218** (2024), 1-19.

[Bar08] I. Bárány, On the power of linear dependencies, in *Building bridges*, Springer, Berlin, 2008, 31–45.

[Ber31] V. Bergström, Zwei Sätze über ebene Vectorpolygone (in German), *Abh. Math. Sem. Univ. Hamburg* **8** (1931), 148–152.

[BD+98] T. Biedl, E. Demaine, M. Demaine, S. Lazard, A. Lubiw, J. O'Rourke, M. Overmars, S. Robbins, I. Strinu, G. Toussaint, and S. Whiteside, Locked and unlocked polygonal chains in 3D, *Discrete Comput. Geom.* **26** (1998).

[CJ98] J. Cantarella and H. Johnston, Nontrivial embeddings of polygonal intervals and unknots in 3-space, *Journal of Knot Theory and Its Ramifications*, **7** (1998), 1027-1039.

[CO01] R. Cocan and J. O'Rourke, Polygonal chains cannot lock in 4D, *Computational Geometry*, **20** (2001), 105–129.

[Con77] R. Connelly, A counterexample to the rigidity conjecture for polyhedra, *IHÉS Publ. Math.* **47** (1977), 333–338.

[CDR03] R. Connelly, E. Demaine and G. Rote, Straightening polygonal arcs and convexifying polygonal cycles, *Discrete & Computational Geometry*, **30** (2003), 205–239.

[DO05] E. Demaine and J. O'Rourke, A survey of folding and unfolding in computational geometry, *Combinatorial and computational geometry* **52** (2005), 167-211.

[Fáry48] I. Fáry, On straight line representation of planar graphs, *Acta Univ. Szeged. Sect. Sci. Math.* **11** (1948), 229–233.

[Gai14] A. A. Gaifullin, Flexible cross-polytopes in spaces of constant curvature, *Proc. Steklov Inst. Math.* **286** (2014), 77–113.

[GG14] A. A. Gaifullin and S. A. Gaifullin, Deformations of period lattices of flexible polyhedral surfaces, *Discrete Comput. Geom.* **51** (2014), 650–665.

[GG+24] M. Gallet, G. Grasegger, J. Legerský, J. Schicho, Pentagonal bipyramids lead to the smallest flexible embedded polyhedron, (2024); https://arxiv.org/abs/2410.13811.

[GP22] A. Glazyrin and I. Pak, Domes over curves, *International Mathematics Research Notices* **2022** (2022), 14067-14104.

[Glu75] H. Gluck, Almost all simply connected closed surfaces are rigid, in *Lecture Notes in Math.* **438**, Springer, Berlin, 1975, 225–239.

[Gol42] M. Goldberg, Polyhedral linkages, *National Mathematics Magazine* **16** (1942), 323-332.

[GZ19] S. Guest, H. Zeyuan, On rigid origami I: piecewise-planar paper with straight-line creases, *Proc. R. Soc.* **475** (2019).

[KM96] M. Kapovich and J.Millson, The symplectic geometry of polygons in Euclidean space, *J. Differ. Geom.* **44** (1996), 479–513.

[KM02] M. Kapovich and J. Millson, Universality theorems for configuration spaces of planar linkages, *Topology* **41** (2002), 1051–1107.

[Kem75] A. Kempe, On a general method of describing plane curves of the nth degree by linkwork, *Proceedings of the London Mathematical Society* (1875), 213-216.

[Ken05] R. Kenyon, *Open problems*, Personal website, https://gauss.math.yale.edu/~rwk25/openprobs/index.html (version: 2024-06-09).

[King99] H. King, Planar linkages and algebraic sets, *Turkish Journal of Mathematics* **23** (1999), 33–56.

[King98] H. King, Configuration spaces of linkages in $\mathbb{R}^n$, (1998); https://arxiv.org/abs/math/9811138.

[Kly96] A. Klyachko, Spatial polygons and stable configurations of points in the projective line, in *Algebraic geometry and its applications, Aspects Math.*, 1996, 67-84.

[Li18] J. Li, *Flexible Polyhedra: Exploring finite mechanisms of triangulated polyhedra*, Ph.D. thesis, University of Cambridge, 2018, 176 pp.; available at https://www.repository.cam.ac.uk/handle/1810/271806.

[Pak09] I. Pak, *Lectures on discrete and polyhedral geometry*, monograph draft (2009); available at http://www.math.ucla.edu/~pak/book.html.

[Poz60] È. Poznjak, Non-rigid closed polyhedra (in Russian), *Vestnik Moskov. Univ. Ser. I Mat. Meh.* **3** (1960), 14-19.

[Sar53] P. Sarrus, Note sur la transformation des mouvements rectilignes alternatifs, en mouvements circulaires, et reciproquement, *Académie des Sciences* **36** (1853), 1036-1038.

[Sta12] R. Stanley, *Enumerative combinatorics*, vol. 1 (second ed.), Cambridge Univ. Press, 2012, 626 pp.

[Stei57] H. Steinhaus, Problème 175, *Colloq. Math.* **4** (1957), 243.

[Stew19] I. Stewart, Tetrahedral chains and a curious semigroup, *Extracta Math.* **34** (2019), 99–122.

[Świ59] S. Świerczkowski, On chains of regular tetrahedra, *Colloq. Math.* **7** (1959), 9-10.

[Tou99] G. Toussaint, Computational polygonal entanglement theory, *Proceedings of the VIII Encuentros de Geometría Computacional*, Castelon, Spain (1999) 269-278.

[WKA16] K. Waldron, G. Kinzel and S. Agrawal, Kinematics, dynamics, and design of machinery, John Wiley & Sons, West Sussex, United Kingdom, (2016), 361-392.

[Wil12] S. Wilson, Embeddings of polytopes and polyhedral complexes, Ph.D. Thesis, University of California Los Angeles, 2012, 95pp.; https://www.math.ucla.edu/∼pak/papers/Stedman-Wilson-thesis.pdf.